KWAME NKRUMAH UNIVERSITY OF SCIENCE AND TECHNOLOGY

Throughput Performance and Coverage Analysis of WiMAX

Network

By

Tetteh, Lord Anertei BSc. ECE (Hons)

PG5903811

A thesis submitted to the

Department of Telecommunications Engineering,

Kwame Nkrumah University of Science and Technology

In partial fulfilment of the requirement for the degree of

Master of Science (Telecommunication Engineering)

Faculty of Electrical and Computer Engineering

College of Engineering

MAY, 2015

Declaration

I hereby declare that this submission is my own work towards the MSc. and that to the best of my knowledge, it contains no material previously published by another person nor material which has been accepted for the award of another degree of the University, except where due acknowledgement has been made in the text.

Tetteh, Lord Anertei ....

Signature Date

Certified by

Dr. James D. Gadze ....

(Supervisor) Signature Date

Certified by

Prof. P.Y. Okyere ....

(Head of Department) Signature Date
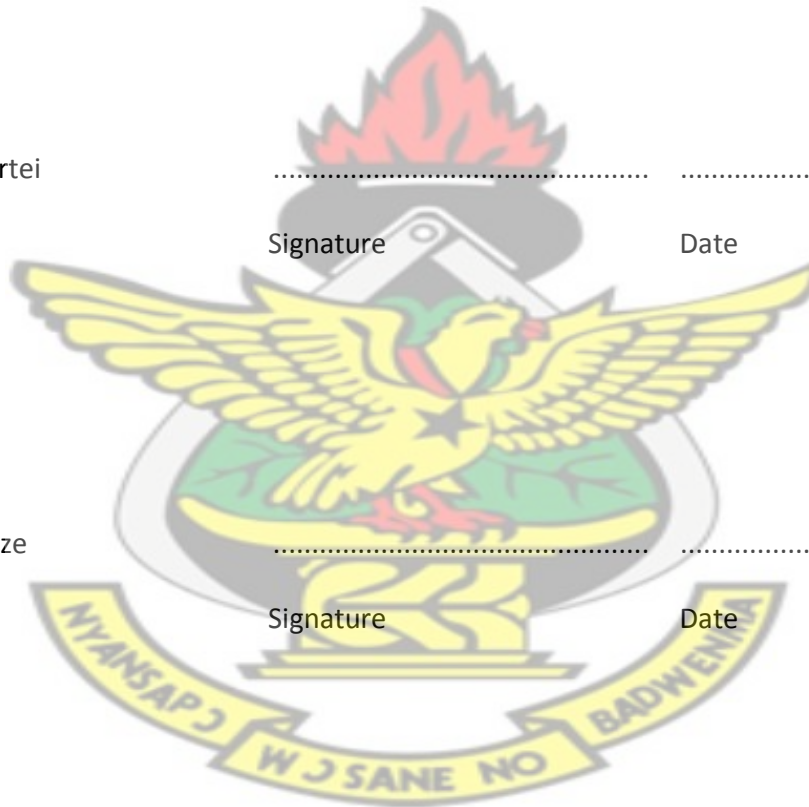
Abstract

The massive increase in radio communication sector and the act of freeing from regulations (especially from governmental regulations, NCA) in the telecommunications industry in Ghana have necessitated the deployment of Worldwide Inter-operability for Microwave Access (WiMAX) in the 2500-2690 MHz band to help serve the ever increasing needs of broadband internet subscribers in the country. This research project seeks to carry out network performance evaluation of a deployed WiMAX network in Accra. In order to achieve our goal of providing comprehensive coverage and throughput measurement that will aid as capital importance in network operators to understand WiMAX performance and provide a guide for future network deployment in Ghana, a realistic physical layer performance evaluation of WiMAX is provided. The performance evaluation is carried out by system parameter measurement campaigns that took place at University of Ghana campus. The physical layer performance of the deployed WiMAX systems is evaluated in terms of measured throughput and received power. This allowed for a direct comparison with simulated results.

Due to inherent system losses, it was realized through the evaluation process that, not even a system with an optimum 4x4 MIMO antenna configuration was able to achieve the simulated throughput of 8.82Mbps. Our measurements established that, we can attain a throughput of approximately 300Kbps downlink and 156Kbps uplink with the most robust modulation scheme, at a maximum coverage range of 4km and a speed of 60km/h, making WiMAX a bright prospect for large-scale deployments in Ghana.

Table of Contents

List of Figures

KNUST

List of Tables

KNUST

Abbreviations

ASN……….. .Access Service Network

AMC…………Adaptive Modulation and Coding

ASN-GW……Access Service Network Gateway

BSC.................Base Station Controller

BSS ....Base Station Subsystem

BS…………… Base Station (same as BTS)

BTS ....Base Transceiver Stations

BER…………Bit Error Rate

BWA……….Broadband Wireless Access

CINR……….. Carrier to Interference plus noise ratio

CSN…………Connectivity Service Network

CPE………….Customer Premises Equipment

DSL…………..Digital Subscriber Line

DL……………Downlink

EDGE…………Enhanced Data Rates for GSM Evolution
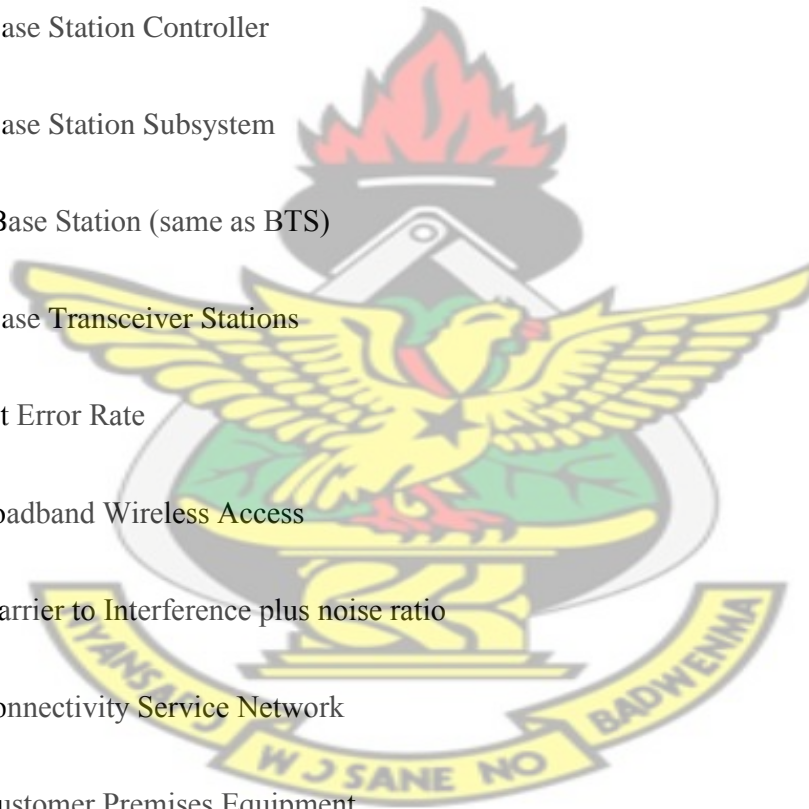
FTP………….File Transfer Protocol

FDD.................Frequency Division Duplex

FFT…………..Fast Fourier Transform

FFR…………..Fractional Frequency Reuse

GPRS……….. General Packet Radio Service

GSM................Global System for Mobile Communications

HSCSD……......High-Speed Circuit-Switched Data

HSDPA………High Speed Downlink Packet Access

HARQ………..Hybrid automatic repeat-request

ISDN ....Integrated Subscriber Digital Network

ISP……………Internet Service Provider

IP…………...Internet Protocol

IEEE………… Institute of Electrical and Electronics Engineers

LTE ....Long Term Evolution

LDPC………...Low-Density Parity Check

MIMO………..Multi-input Multi-output

MS..................Mobile Station

MUD……….. Multiuser Detection
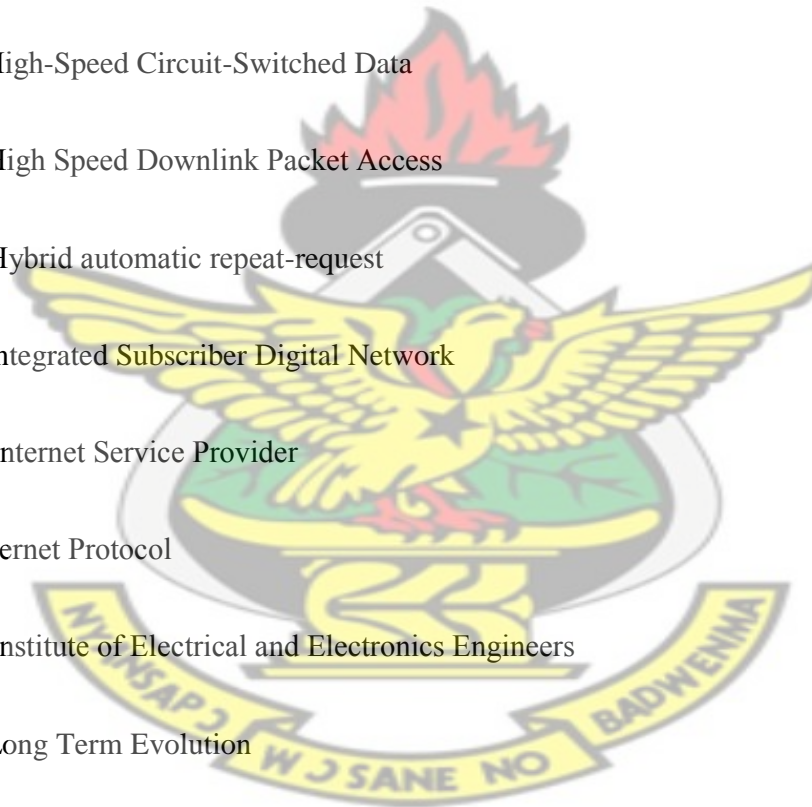
MSC ....Mobile Services Switching Centre

NITA…………National Information Technology Agency

NRM………...Network Reference Model

OFDM………..Orthogonal frequency division Multiplexing

PUSC…………Partial Usage Subcarrier

QoS…………..Quality of Service

RF....................Radio Frequency

RSS………….Receive Signal Strength

SNR………… Signal to Noise Ratio

SOFDMA……..Scalable OFDMA

SU ....Subscriber Unit

SS……………Subscriber Stations

SMS.................Short Message Service

SISO………...Single Input Single Output

3GPP…………3rd Generation Partnership Project

QAM………..Quadrature Amplitude Modulation

QPSK……….Quadra phase shift keying

UL…………..Uplink
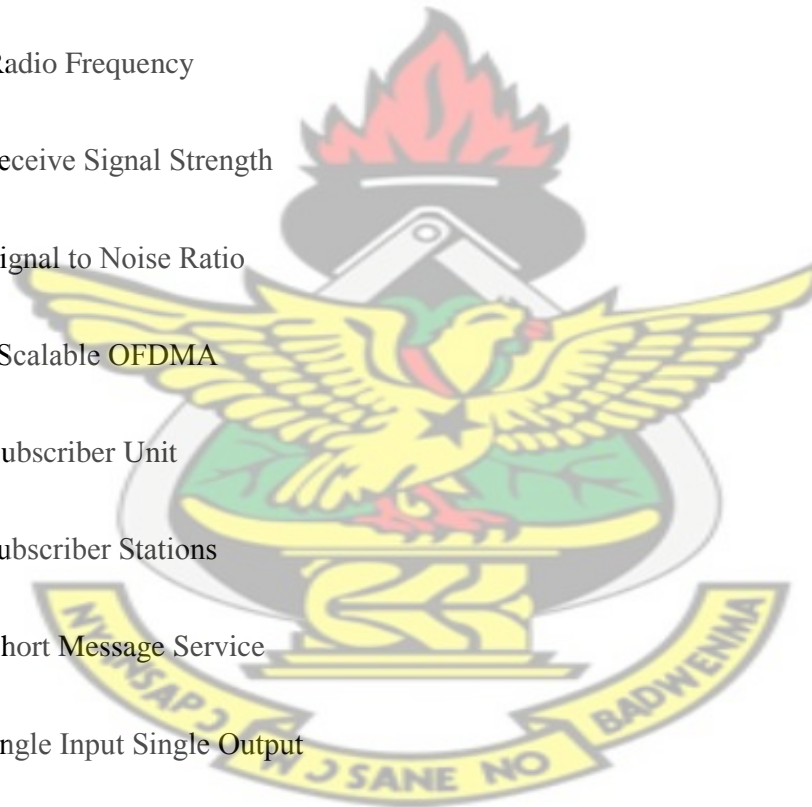
UMTS……….Universal Mobile Telecommunications System

VoIP………..Voice over Internet Protocol

WiMAX ....Worldwide Inter-operability for Microwave Access

WLAN………..Wireless Local Area Network

Dedications

This research is dedicated firstly to Jehovah God Almighty, secondly to my family and lecturers of the

Kwame Nkrumah University of Science and Technology.

Acknowledgement

So soon our study for the Master of Science in Telecommunication has come to an end without living any stone unturned. The struggle was tough and hard yet I kept my focus on the joy of completing the course for the past two (2) years at the Kwame Nkrumah University of Science and Technology.

I, very much acknowledge the Grace and Protection of the Almighty God for guiding and helping reached my target of the successful completion of the course. I recognize the sacrifice and support of families.

I also thank my supervisor, Dr. James Gadze for the direction and supervision to finish this project, not forgetting Eric Tutu for his enormous contributions.
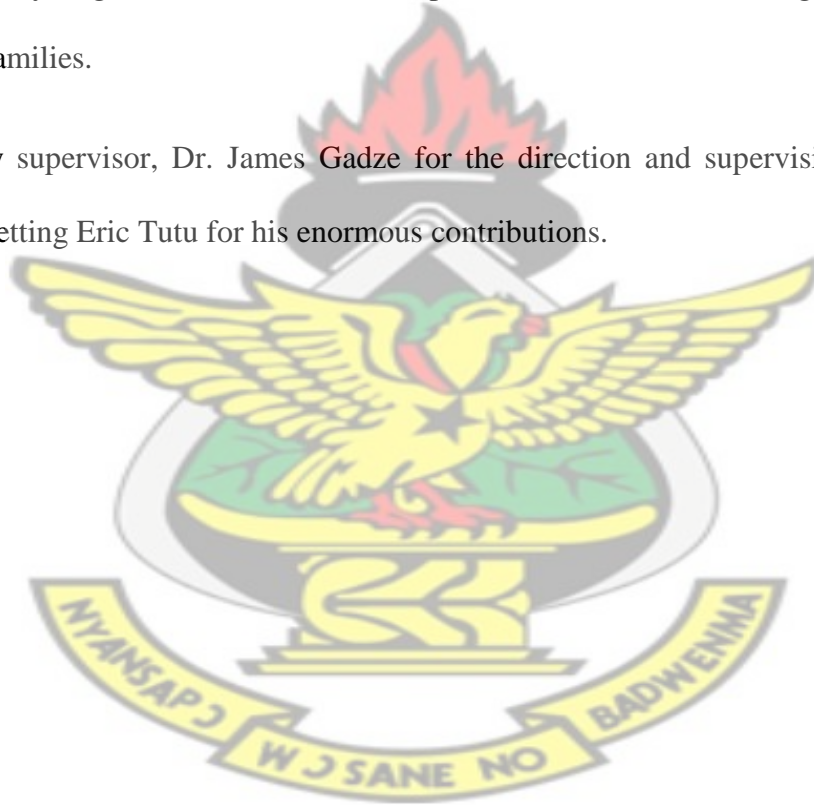
Chapter One: Introduction

1.1 Background and Motivation

In recent world, broadband wireless access (BWA) is the new wireless technologies are allowing us into an age where information becomes geographically as well as personally. Broadband internet access helps to shape, self-centered, and evolution-oriented information, where everybody can create, access, share information and enable communities to achieve their quality of life [1].

There has been an increased in the demand for broadband internet access for small office/home office (SOHO), and small- to medium-enterprise (SME) markets. This has led to internet service providers (ISP) looking to other ways in which to deliver their service to the consumer (last mile). This has led to a re-haul in thinking between the traditional methods of wired technology and wireless technology [2].

The main business concern of these ISP's, is how many economic consumer's they can support at each time in a given area and the parameters to be used. This need elaborated simulation work.

What this paper seeks to achieve is to present measurement values from life WiMAX deployed in Accra together with comprehensive analyses and compare with simulation models.

WiMAX equipment has been deployed by many network operators across the globe for interoperability testing [2]. WiMAX Mobile broadband wireless technology has rapidly gained support on the IT market among network providers and telecommunication equipment manufacturers. However, evaluation of WiMAX technology offering exponentially greater range and throughput performance in realistic system deployment scenarios is difficult because of the different subscriber station (SS) configurations, path loss, shadow fading and system loading which should be factored in the System Level Simulation methodology.

In Ghana, Digital Subscriber Line (DSL), which was the main technology for providing broadband internet, is quite expensive and as such there is a need to find an affordable technology which will provide a platform for the least privileged to have access to broadband internet access even at a distance of many kilometers from his/her home. There are several wireless broadband technologies but WiMAX offers a platform which provides increased coverage and low-cost services [3]. Wireless Broadband internet service is very expensive in many countries sub of Sahara and because of this only the rich can have access to high speed internet access. Since WiMAX promises last mile broadband solution at cheaper cost, many countries in sub Saharan Africa including Ghana, have prepared the spectrum in the 2.5GHz-2.690GHz for auction to enable the least privileged to benefit from this high capacity technology [4].

WiMAX is to provide users in rural areas (last mile) with high speed data communications as an alternative for expensive wired connections (DSL) [5].

On per user frame basis, WiMAX supports different modulation schemes and allows the scheme to be changed, based on communication medium conditions. Adaptive Modulation and Coding (AMC) is efficient in maximizing throughput in a time varying channel as well as coverage.

The algorithmic rule typically calls for the use of the highest modulation and coding scheme that can be backed by the SNR and CINR at the receiving end such that each user is offered with the highest data rate that can be supported in their respective connections. This makes it possible to offer home and business user's high speed internet rates at even a distance far from the base station.

WiMAX infrastructure is less expensive to deploy as compare to the cable network or the DSL, this simply should lead to more ubiquitous broadband access [6].

WiMAX is reported as a standard technology by WiMAX forum which enable data delivery to the last mile, therefore it is a substitute to cable networks and DSL. Knowing that WiMAX has been developed for this very purpose, there is a need to test the performance of this technology since it will help the least privileged enjoy affordable broadband services. This research seeks to perform simulation and field trial measurement for a deployed WiMAX BS in Accra and make performance comparison between Simulated and measured results.

1.2 Problem statement

WiMAX is a promising new technology with much theoretical standards and performance expectations [7]. WIMAX promises last mile broadband solutions to the least privileged and as such it is expected that WiMAX will help solve Africa's problem of inadequate internet access. However, subscribers in Ghana especially, are therefore keenly expecting high performance and as such it is very relevant to evaluate the performance of a newly deployed WiMAX Base Station in Accra to determine how WiMAX performs under the peculiar conditions in Ghana.

1.3 General Objectives

The general objective of this work is to determine the throughput performance and coverage analysis of WiMAX Base Station through capacity simulation and field trial measurements. An appropriate simulation tool will be used for estimating per sector capacity and coverage of the Base Station for specified deployment scenarios.

The research seeks to use numeric features obtained by system level simulations (SLS) to evaluate the coverage and throughput capacity of the WiMAX network deployed in Accra. This work will outline the main simulations parameters and infrastructures of 802.16e WiMAX PHY, simulations scenarios and assumptions such as path loss models, frequency reuse, system loading, and subscriber stations placement.

1.4 Specific Tasks

The research will use scientific methods and appropriate simulation and evaluation tools to achieve the following specific Objectives:

1. To determine the achievable average per sector throughput in the cell using adaptive Multi-Input Multi-Output (MIMO) antenna configurations.

2. Perform link budget for the WiMAX Base Station for specific deployment scenarios.

3. Take Real field measurements in a deployed cell site and compare with the simulated values.

1.5 Significance

WiMAX provides broadband solution with various applications, which has several advantages such as the acceptance of advanced radio communication features in a uniform fashion to cut down costs for all of the radios made by companies who are belong to the WiMAX Forum. WiMAX in no doubt, help bridge the ever increasing digital gap in Ghana.

The WiMAX Base Station under study has been deployed to offer Ministries, Departments and Agencies (MDAs) affordable broadband internet service. Because of the harsh terrain and other conditions in Accra, an evaluation of this Base Station will help in knowing which parameters have to be optimized to enable the WiMAX networks deliver as highly expected by subscribers. Moreover, in order to attain maximum throughput capacity while keeping an acceptable grade of service (GOS) and a higher network performance to help this deployed BS to achieve the

objective of reaching all MDAs in the cell, the parameters used in planning this network should be evaluated and optimization techniques proposed.

This will provide alternate optimised designs for the WiMAX network, to ensure that the network will serve the widest possible diversity of MDAs as well as Quasi-Government Institutions, Organisations, and Corporations.

Knowledge of evaluation process and capacity estimation is key to meet the demand on Wireless technologies. Since Wireless technology has proven itself to be a fast evolving technology, from the entry of GSM and WLAN to third generation mobile technology and lately Long Term Evolution(LTE), this research project will provide knowledge for Network planning engineers in Ghana to plan WiMAX networks to be able to meet subscriber's continuously increased demand for mobility, services and capacity. The research will give an insight into considerations for a typical WiMAX deployment in Ghana. The research also gives guidance to RF Engineers, data carriers and Internet Service Providers (ISP) on how well they can plan their networks for wireless transmission.

1.6 Limitations to the study

The project described in this document suffered from some constraints. Of significant mention is

1. Inaccessibility to digital maps

2. Relevant simulation and radio planning software due to proprietary and confidential reasons.

3. Some of the network operator's refused to disclose certain network parameters and it's also worrying.

4. Real-life deployed network was used during the work.

1.7 Organization of thesis

This work has five chapters:

Chapter One: Introduces the work: it presents the motivation and objectives of this work. This sets the stage for the chapters that follow.

Chapter Two: Gives a review of relevant literature and a brief introduction to the WiMAX network reference model and the PHY layer.

Chapter Three: The System Level Simulation methodology used in this work is thoroughly discussed. The propagation environment and the key parameters used in the coverage and capacity simulation for deploying the WiMAX BS is subsequently defined.

Chapter Four: This section describes the simulation model adopted for analyzing the capacity and coverage range of the deployed WiMAX network. The simulation results and field experimental data is presented and analyzed.

Chapter Five: Contains conclusion and general recommendation as to how the results obtained can be used and areas of refinement and further study.

Chapter Two: Literature Review

2.1 Introduction

In 1991, the Global System for Mobile communications (GSM) was commercially launched, which has been the first fully digital mobile communication system. In September 2012, estimated three billion people (or 80% of the total world-wide subscribers) were connected by GSM [8]. However, GSM in its original form only allowed the user's to make and received calls as well as send text messages through (SMS). After data transmission techniques like HSCSD, GPRS, and EDGE were introduced into the GSM network this changed [9]. With a single time slot per frame allocated to a subscriber, the data rate supported by HSCSD is 14.4kbit/s. Using GPRS it is 22.8kbit/s and with EDGE 68.4kbit/s. By using multiple time slots, the maximum data rate can be raised accordingly [10].

When Universal Mobile Telecommunications System (UMTS) was launched, the first mobile communication equipment was available that supported wireless data transmission already in the first released version. By using spreading factors of variable length, the data rate in UMTS could be adjusted up to a maximum of 384kbit/s. On the contrary, HSDPA, introduced by the third Generation Partnership Project (3GPP) around 2002, as an extension to UMTS, uses spreading factors of fixed length while adjusting the data rate by the combination of AMC [11] and the number of spreading codes assigned to the subscriber. The current passage condition required by AMC is reported by the receiver to the transmitter in regular time intervals. The HSDPA user equipment's are classified into several categories depending on the maximum code-block length and the maximum symbol alphabet size supported.

Another important feature of HSDPA, introduced with 3GPP Release 7 in the year 2007, is Multiple Input Multiple Output (MIMO) operation. Two transmit antennas are deployed at the base station to enable spatial pre-coding with the objective of enhance the Signal to Noise Ratio (SNR) at the receiver's end. If two receive antennas are available at the user equipment as well, two spatially separated information can be transmitted simultaneously. Although implementation of the MIMO capability is an additional cost for the network operator, the enhancement in spectral efficiency should —at least in theory— make up for that.

Between Release 5 (2002) and Release 7 (2007) which were issued by 3GPP, the Institute of Electrical and Electronics Engineers (IEEE) worked on standardization from 802.16-2004 [3], often referred as Worldwide Inter-operability for Microwave Access (WiMAX). The criterion was developed for delivering (last mile) broadband Internet as a substitute to cable network or Digital Subscriber Line (DSL). Like HSDPA, WiMAX also supports AMC and MIMO. Multiple transmit and receive antennas are integrated in standard by Alamouti space time coding [4].

With exponential increase in data demand, Wireless broadband technologies like WiMAX, LTE, 3G+, etc. have made it possible for people to enjoy broadband internet access, telephone call when they are fixed or roaming terms.

The rapid growth in broadband internet causes an exponential call for high data speed access to the internet services. In other to serve this demand, "anywhere, anytime" and ensure quality of service, deployment of these wireless broadband systems have already started in many parts of the world. However, many countries in Africa have just recently started WiMAX deployments to deliver broadband internet access to subscribers.

This chapter introduces the WiMAX Standard, Network Reference Model and a review of related work done in evaluating WiMAX networks.

2.2 Review of Related Literature

With the ever-increasing need for mobile communication and the emergence of many systems, it is important to design WiMAX networks that will conform to the performance it promises. There have been numerous interference simulation studies and field measurement trials of WiMAX base station which involves system coverage, signal strength and available transmission rate done in Europe and Asia.

In [15], real time images and Voice over IP (VoIP) are transmitted through Skype software by using WiMAX deployed in the 2.5GHz-2.69GHZ band, and this information are connected to exchange wireless monitoring servers to execute data monitoring and analysis. Comparison analysis was then made and the maximum measured throughput was 3.86Mbps as compared to the simulated throughput of 10Mbps. From the measurement trials in [16] it was realized that the real field performance was different from the documented performance. At about 1km away from the BS, the network connection dropped. Even though higher throughputs were measured up to about 1km away from the Base station (BS), the BS couldn't help deliver WiMAX promise of providing last mile broadband solution.

In [17] an evaluation was carried out on a 3.5MHz channel bandwidth typical for the 3.5GHz WiMAX band in Europe. The maximum measured downlink and uplink throughput were 8.9Mbps and 11.95Mbps respectively. Measurements were taken from 95 out of 152 locations and the results analyzed. All fact-finding configurations indicated a moderate correlation

between network performance, distance and Carrier to Interference plus noise ratio (CINR). A model relating to the Critical CINR to measured data rate was developed that greatly helped WiMAX operators in Europe to enhance network performance.

In [18], the measurement was conducted on WiMAX Bases stations operating in the 2360-2390MHz band at Cyberjaya, Malaysia, and the propagation path loss exponent was modeled. The WiMAX Base station selected was 23m above ground level. This site has four WiMAX Base Stations which transmitted in vertical polarization. The main contribution in the research work was the optimization of the Hata model based on the frequency of 2375MHz.

In [19], Analytical cell load calculation was proposed. A linear estimation is used to capture the behavior of AMC by adapting the effective data rate of a user channel quality. Hence, it gives a system of linear equations and conditions for the total channel activities and service probabilities of the cells, which qualify the cell loads. In [20], Optimization of antenna tilt, azimuth, and transmission power resulted in substantial betterment in network performance when comparing to the Signal interference plus noise (SINR), Cumulative density function (CDF) of optimized designs with that of the master design.

A traditional study approach was used to do characteristic and sharing analysis, as depicted in Draft CEPT Report 019 [20]. This approach path is based on the governed minimum technical performance parameters which all equipment suppliers are compelled to meet. Following the governed minimum technical standards for the study can lead to unduly negative isolation margins. Therefore, the ITU Report [21], follows the analytical results with results of statistical analysis that leads to a modeled system performance averaged over the population of users.

In [22], additional isolation showed improved performance both in the coexisting and the co-location of WiMAX and LTE systems scenarios. In [23], the efficient approached for both aspects of the cosite prediction challenge, was addressed. A tool was developed for effective management of multi-fidelity models for executing cosite interference predictions.

Field trial experiments carried out by authors in [25] showed a wide disparity between the coverage promised by WiMAX in two separate deployment scenario. It is worth mentioning that all the measurements and simulation works done in these studies were done in USA, Europe and Asia as stated before. From [24][25], it has been established that environmental conditions play an important role in network performance, it is imperative for us to do an independent evaluation of WiMAX Base Station deployed in Ghana to come out with the correct performance parameters pertinent to Sub- Saharan environment to enable our network operators effectively deploy WiMAX to afford subscribers the chance to benefit from this open standard.

2.3 WiMAX Standard

In 2001, the WiMAX forum introduced the first fixed Standard 802.16 with line of sight (LOS) demand, which uses a single carrier frequency with 10-66 GHz spectrum support. This basic standard allows for theoretical rates of up to 134Mbps. In January 2003, 802.16a standard was approved with a non-line of site (NLOS) which support 2-11GHz frequency, where the first orthogonal frequency division Multiplexing (OFDM) and the mesh mode were added to the WiMAX system.

The 802.16 b & c were amended to the 802.16a and all of them were theoretical standards which later were grouped in the 2004 WiMAX standard 802.16d. The 802.16d known as the first fixed working standard of WiMAX supports data rates of up to 70Mbps, uses 256 point fast Fourier transform for Orthogonal Frequency Division Multiplexing (OFDM) and 2048 points transform OFDMA (OFD Multiple Access)[12]. In 2005 [13], the mobile WiMAX IEEE 802.16e was introduced with the following melioration over previous standards:

1. It endorses mobility by introducing a Mobile Stations (MS) instead of Subscriber Station (SS). MS in this standard can stay connected during movement from one Base Station (BS) coverage area to another BS coverage area through efficient handover procedures.

2. It uses Scalable OFDMA (SOFDMA) technology to increase spectrum efficiency and reduce cost in wide and narrow band channels. It obtains this scalability by allowing dissimilar FFT point values for each channel width to result in a fixed carrier spacing.

3. It uses the advance antenna technology supporting the Multiple Input Multiple Output MIMO technology.

4. It uses the downlink sub-channelization, allowing decision maker to trade coverage for capacity or vice versa.

In 2009, WiMAX forum approved the 802.16j called the MMR mode that is just an extension to the original PMP. MMR mode have a tree structure where intermediate subscriber stations can work as relays to forward traffic and is fully backward compatible with 802.16e standard [14]

2.4 WiMAX Network Reference Models

The WiMAX forum has presented ordered representation of the network architecture for WiMAX which is known as "Network Reference Model" (NRM). The NRM has operational entities and reference points where interoperability functions are defined.

Figure 2.1 below shows the NRM which consists of mobile stations (MS), access service network (ASN) and connectivity service network (CSN). It also defines the Reference Points R1-R6 and R8 as shown in Figure 2.1 [13]
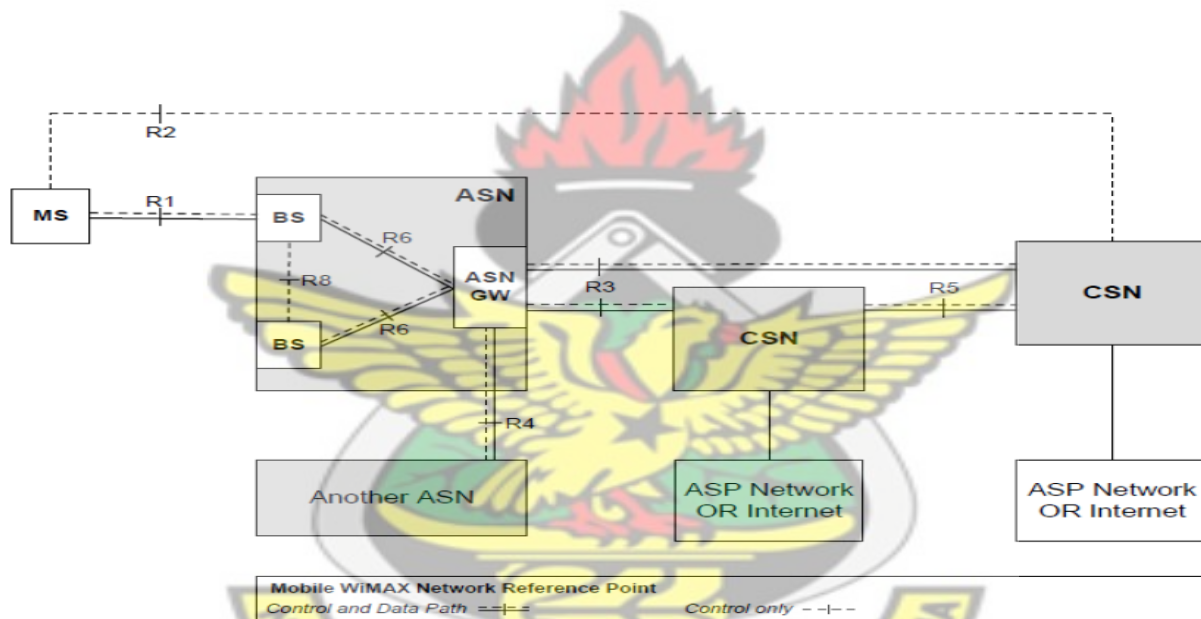

Figure 2.1 WiMAX reference model.

It may be that these entities work in an individual physical function or it might be distributed over multiple physical roles. ASN comprises of one or more base station(s) and at least one access service network gateway (ASN-GW).

The primary aim of the NRM is to use multiple effectuation options for a given functional entity and achieve interoperability among different logical entities. Interoperability depends on the communication protocols and the flow of data between the logical entities to achieve an overall end to end function like security and mobility management.

Functional entities have reference points with which they are connected and it includes control and data path end points. Interoperability is based only on protocols exposed across an RP, which depends on the end to end functions. Thus the information on NRM makes the optimal use of protocols over an RP to support the capability. If the implementation supports the capacity and exposes the RP, then the implementation shall comply with this specification. Hence it avoids the situation where protocol entity can reside on either side of an RP or the replication of identical procedures across multiple RPs for a given capability. Both the IP services and the Ethernet services are supported by the network reference model with all its reference points.

A reference point is a logical point between the two groups of entities that reside on either side of it. These functions are related to protocols related with the RP. It could be observed that these protocols associated with the RP might not terminate in the same functional entity that is, there is a possibility that two protocols are associated with a RP and they might start and end in different functional entities.

According to the WiMAX forum mobile system profile, the reference point R1 consists of the protocols between the MS and the BS of the ASN as per the air interface specification. R1 can also include additional protocols related to the management plan.

The MS and the CSN, lies the reference point R2 where authentication, service authorization and IP Host Configuration management protocols and procedures are included. This reference point is considered to be logical because it doesn't depict a direct protocol interface between MS and

15

CSN. The reference point R2 that runs between the MS and the CSN operated by the home Internet Service Provider (ISP) includes the authentication part and IP Host Configuration Management is supported by reference point R2 running between the MS and the CSN operated by either the home or the visited ISP. R2 between ASN and CSN operated by visited CSN may partially process the procedures and mechanisms.

A set of control protocols between the ASN and the CSN to support Authentication, Authorization, Accounting, policy enforcement and mobility management capabilities are controlled by a logical connection known as reference point R3. It also includes the data path methods like tunneling to transfer the user data between the ASN and CSN.

A set of control and data path protocols starting and ending in an ASN-GW that synchronizes MS mobility between ASNs and ASN-GWs is supported by Reference point R4. R4 is solely responsible for interoperable function between the ASN-GWs of one ASN or two different ASNs. The reference point that supports a set of control and data path protocols for interoperability between the CSNs operated by the home ISP and that operated by a visited ISP is the R5.The reference point that controls the set of control and data path protocols for communicating between the BS and the ASN-GW within a single ASN is R6. It is an intra-ASN data path between the BS and ASN-GW. The control plane function comprises of data establishment, modification and release control in accordance with the MS mobility events. Reference Point 7 is a logical entity within the ASN-GW and represents internal communication within the gateway. Reference Point R8 is for intra-ASN and consists of the set of control plane messages between the base stations for fast and seamless handover. It contains the inter-BS communication protocol with the WiMAX forum Mobile System Profile and other set of

protocols that allow controlling the data transfer between the Base Stations involved in handover of a certain MS.

2.4.1 ASN Reference Model

Access Service network ASN comprises of ASN-GW(s) and Base Station(s) which performs functions to provide access service. The ASN has R1 reference point with an MS, R3 reference point with a CSN and R4 reference point with another ASN-GW. The ASN has at least one Base Station (BS) and at least one ASN Gateway (ASN-GW) as shown in Figure 2.2 [13].
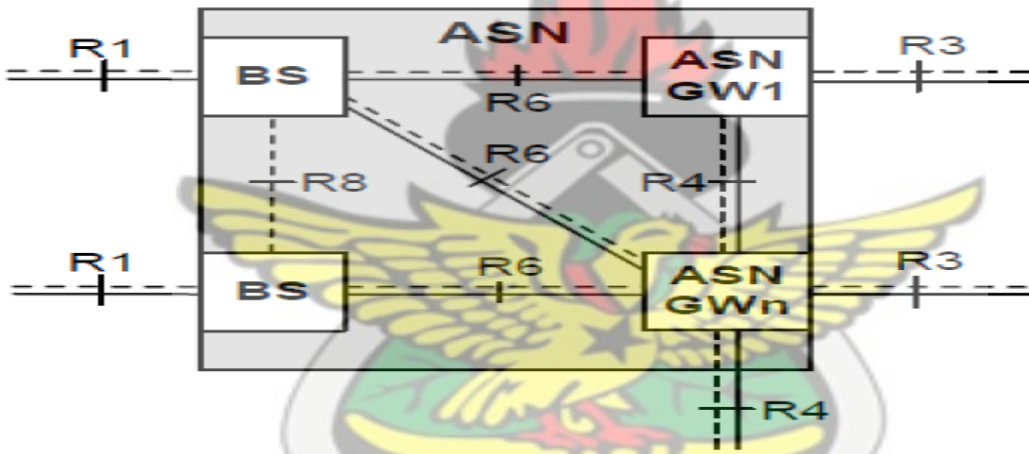
Figure 2.2 Reference model

One Base Station may be connected to several ASN-GW for different MS. When it comes to one MS then BS is connected to a single ASN-GW. The Base Station is the logical entity that encompasses a full layer of WiMAX MAC and PHY layer with compliance to IEEE 802.16 applicable standards and may also perform one or more access functions. A WiMAX BS is assigned one frequency with coverage area of one sector. It performs scheduler functions for uplink and downlink and this is completely dependent on the vendors for which scheduling technique is to be used. It may happen that in order to balance the load during hand-offs, a single

17

BS may be connected to more than one ASN-GW. Thus BS is a logical entity and there can be multiple implementations of physical BSs.

ASN Gateway is a logical entity which represents an aggregation of Control plane functional entities that work together with a corresponding function in the ASN perhaps BS, a resident function in the CSN or with a function in a bother ASN. The ASN-GW performs Bearer Plane functions of routing and bridging.

ASN-GW also includes function like redundancy and load balancing with several ASN-GWs for multiple MSs Hand-offs. For one MS, the BS is responsibly connected or associated with only one default ASN-GW. But, internally the ASN-GW functions for every MS among multiple ASN-GWs located in one or more ASN(s).

2.5 Overview of WiMAX PHY

The main reason for the development of wireless broadband is the practical acceptance and cost effective carrying out of an Orthogonal Frequency Division Multiple Access (OFDMA). Today, almost all upcoming broadband access technologies including Mobile WiMAX and LTE use OFDMA. For performance evaluation of WiMAX, it is important to understand OFDMA. Therefore, this section provides us with a very brief explanation that helps introduce the simulation parameters that are used later in the analysis.

Unlike, Wi-Fi and many cellular technologies which use fixed width channels, WiMAX allows almost any available spectrum width to be used. Allowed for channel bandwidths vary from 1.25 MHz to 28MHz. The channel is divided into many equally spaced subcarriers [15]. For example, a 10 MHz channel is divided into 1024 subcarriers some of which are used for data transmission while others are set aside for monitoring the quality of the channel (pilot subcarriers), for

providing safety zone (guard subcarriers) between the channels, or for using as a reference frequency (DC subcarrier).

The data and pilot subcarriers are modulated using one of several available Modulation and Coding Schemes (MCS). Quadrature Phase Shift Keying (QPSK) and Quadrature Amplitude Modulation (QAM) are examples of modulation methods.

In conventional cellular networks, the downlink, base station (BS) to mobile station (MS) and uplink (MS to BS) use different spectrum. This is called Frequency Division Duplexing (FDD). Mobile WiMAX allows not only FDD but also Time Division Duplexing (TDD) in which the downlink (DL) and uplink (UL) share the same frequency but interchange in time [16].

The transmission consists of frames as shown in Figure 2.2 [16].The DL sub frame and UL sub frame are separated by a Transmit to Transmit Gap (TTG) and Receive to Transmit Gap (RTG). The frames are shown in two dimensions with frequency along the vertical axis and time along the horizontal axis.
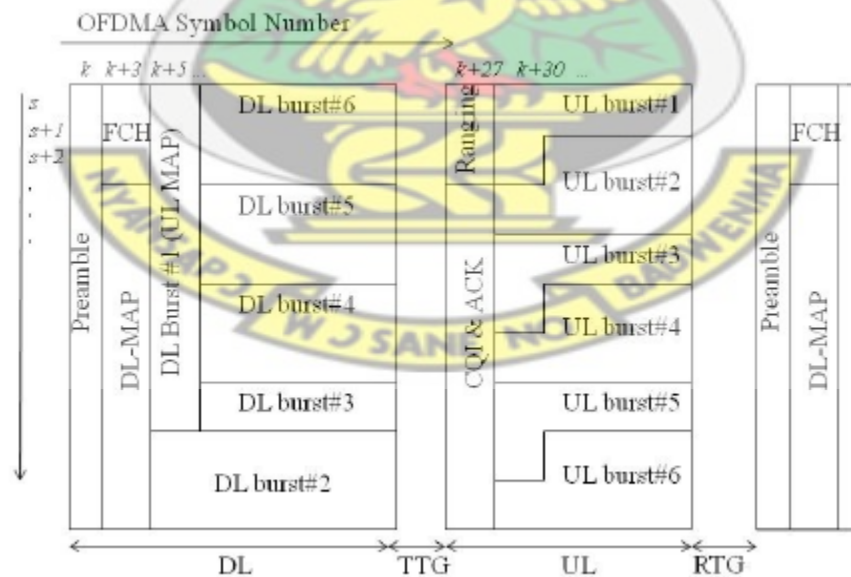

Figure 2.3 Sample OFDMA Frame Structures [16]

In OFDMA, each MS is apportioned only a subset of the subcarriers. The available subcarriers are grouped into a few sub-channels and the MS is allocated one or more sub-channels for a defined number of symbols. The mapping out process from logical sub-channel to multiple physical subcarriers is called a permutation. Basically, there are two types of permutations, distributed and adjacent. The distributed subcarrier permutation is suitable for mobile users while adjacent permutation is for fixed users. Of these, Partially Used Sub-channelization (PUSC) is the most commonly used in a mobile wireless environment [17]. Others include Fully Used Sub-channelization (FUSC) and Adaptive Modulation and coding (band-AMC). In PUSC, subcarriers forming a sub-channel are selected randomly from all available subcarriers. Thus, the subcarriers forming a sub-channel may not be adjacent in frequency. Users are apportioned a variable number of slots in the downlink and uplink. The exact definition of slots depends upon the sub channelization method and on the direction of transmission (DL or UL). Figures 2.4 and 2.5 show slot formation for PUSC [18].

In uplink a slot consists of 6 tiles where each tile consists of 4 subcarriers over 3 symbol times. Of the 12 subcarrier-symbol combinations in a tile, 4 are used for pilot and 8 are used for data. The slot, therefore, consists of 24 subcarriers over 3 symbol times. The 24 subcarriers form a sub-channel. Therefore, at 10 MHz, 1024 subcarriers form 35 UL sub-channels. The slot formation in downlink is different and is shown in Fig. 2.4. In the downlink, a slot consists of 2 clusters where each cluster consists of 14 subcarriers over 2 symbol times. Thus, a slot consists of 28 subcarriers over two symbol times. The group of 28 subcarriers is called a sub-channel resulting in 30 DL sub-channels from 1024 subcarriers at 10 MHz.
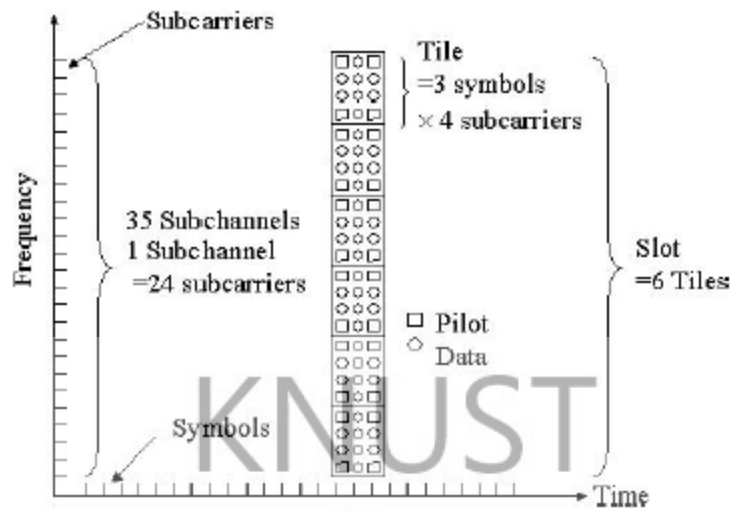
Figure 2.4. Symbols, Tiles, and Slots in Uplink PUSC.
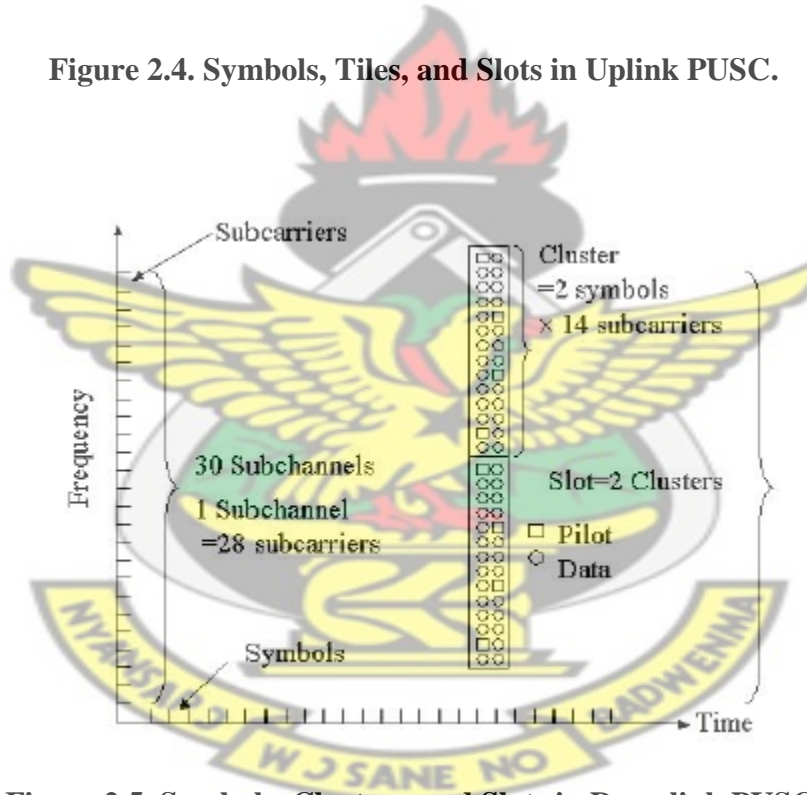
Figure 2.5. Symbols, Clusters, and Slots in Downlink PUSC.

The WiMAX DL sub-frame starts with one symbol-column of preamble. Other than preamble, all other transmissions use slots as discussed above. The first field in DL sub-frame after the preamble is a 24-bit Frame Control Header (FCH). For high reliability, FCH is transmitted with

the most robust MCS (QPSK 1/2) and is repeated 4 times. Next field is DL-MAP which specifies the burst profile of all user bursts in the DL sub-frame. DL-MAP has a fixed part which is always transmitted and a variable part which depends upon the number of bursts in DL sub-frame. This is followed by UL-MAP which specifies the burst profile for all bursts in the UL sub-frame. It also consists of a fixed part and a variable part. Both DL MAP and UL MAP are transmitted using QPSK1/2 MCS.

2.6 Limitations of other technologies
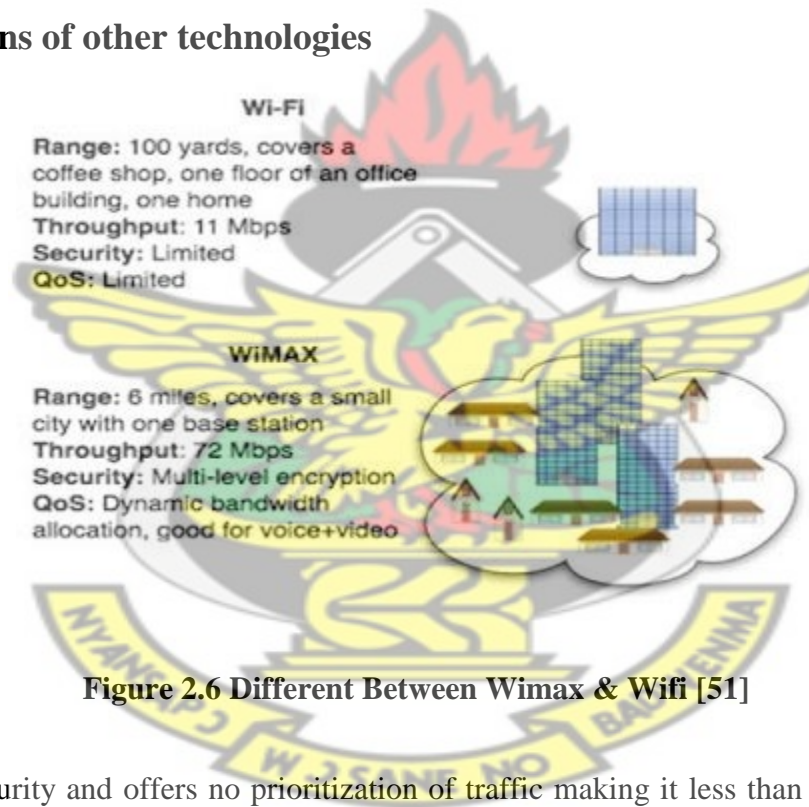
Figure 2.6 Different Between Wimax & Wifi [51]

Wi-Fi lacks security and offers no prioritization of traffic making it less than ideal for voice or video.

In order to cover the same area and provide services to the same number of customers as one WiMAX base station, Wi-Fi service provider must deploy multiple access points.

The throughput capabilities of WiMAX have a selectable channel bandwidth from 1.25MHz to 28MHz, which allows for a very flexible deployment. When deployed using the more likely 10MHz TDD (time division duplexing) channel, assuming a 3:1 downlink-to-uplink split and 2 x 2 MIMO, WiMAX offers 46Mbps peak downlink throughput and 7Mbps uplink. . Unlike 3G systems, which have a fixed channel bandwidth.

In the business circles, there is demand for symmetrical T1/E1 services that cable and DSL have so far not got the technical requirements for. Conventional telecom services continue to serve this demand with relatively little competition. Fixed broadband solutions using WiMAX could potentially compete in this market and trump landline solutions in terms of time to market, cost, and dynamic provisioning of bandwidth.

In summary, WiMAX occupies a somewhat middle ground between Wi-Fi and 3G technologies when compared in the key dimensions of data rate, coverage, QoS, mobility, and price.
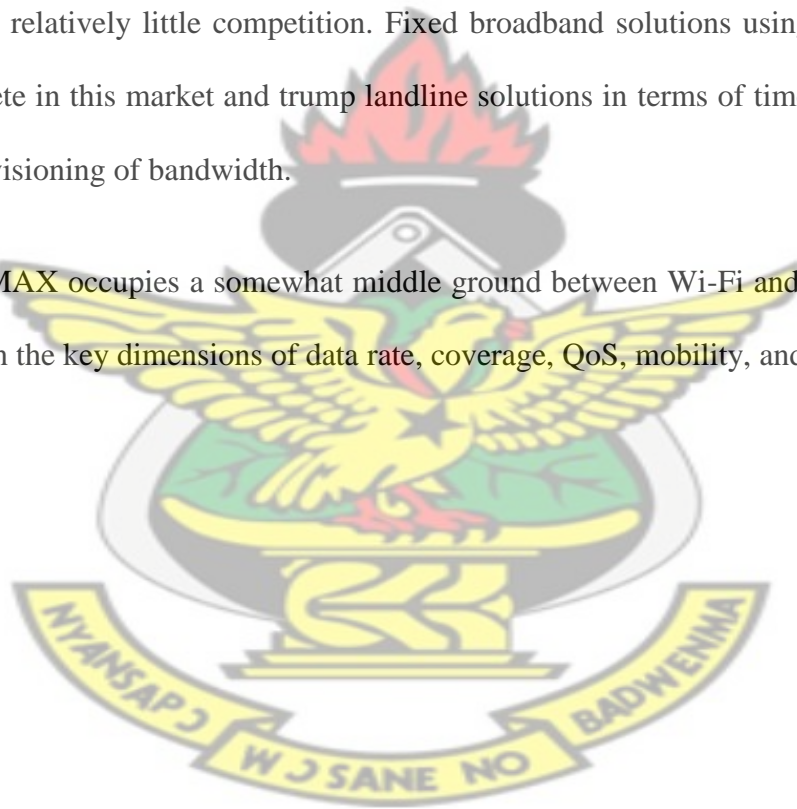
Chapter Three: System design, Modelling and Simulation

3.1 Introduction

This chapter discusses the propagation environment and the key parameters used in the simulations for the WiMAX network under evaluation. The IEEE 802-16e 2005 standard for WiMAX is a accumulation of different standards mainly centered on PHY and MAC layers applications with the objective of providing interoperability between different system specifications. Thus, a high level of tractability is considered in each application. Above all, those are related to access provision such as resource allotment and scheduling process, are designed significantly flexible. So a precise system performance simulation is hardly achievable. In addition, the dynamic channel allocation and scheduling makes it difficult to introduce a practical capacity and coverage estimation procedure.

Furthermore, the number of signaling overhead is not constant and changes with the number of users is unpredictable. In other words, as the subscribers may have dissimilar capacities in their supporting technologies the needed signaling procedure is different from one subscriber to the other in both DL and UL. Since the system supports different QoS specifications, different service provision methodologies are used in resource allocations and scheduling processes on a subscriber based manner.

Moreover, the main reason for element in network planning is to estimate the number of users that each BS may support. But, since the WiMAX networks have not been deployed on a large

scale in Ghana, the user demands cannot be clearly determined and modeled for in this thesis. Considering all the limitations above the actual average throughput calculation seems to be extremely difficult to simulate.

In spite of this limitations, an acceptable approximation for the network capacity in both downlink and uplink directions based on the distribution of existing users on the network will be done. Some basic assumptions for the Bit Error Rate, Coverage and Capacity estimations have been presented in this chapter.

3.2 Propagation Model

The Normal propagation modeling include

1.   Physical models: This model path loss makes use of physical radio waves precepts such reflection or optical phenomenon.

2.   Empirical models: This models use measurement data. ITU-R and the Hata models are examples [26].

Path loss anticipation is very crucial part of system design in telecommunication as the environment of deploy base station invariably changes. The main challenge is always how to estimate the path loss with supreme accuracy. A very good Propagation model is the main style to adopt. A standard model to be use is the one which estimate the path loss with insignificant standard deviation. When this is achieve, very good cell coverage range and the required transmitted power is used by network engineers.

The option of model to be used depends on the propagation environment and the area of coverage. Propagation happens through multiple optical phenomenon, reflection and dispersion etc, from a very large different number of obstacles. Because it is very hard to trace scattering and characterization of the signal within the coverage area, it's done statistically. Based on this, models for path loss prediction have been design using pragmatic or numerical methods. The precision of a particular prediction model in a given environment depends upon the appropriate parameters required by the model and those available for the area concerned [26].

3.2.1 Free Space Propagation Model

When there is no any obstruction between the transmitter and the receiver, then the free space model is used to measure received signal strength (RSS). Free space model calculates received power decays as a function of the Transmitter-Receiver separation distance raised to some power. Friis free space equation is the power from a transmitter to a receiver antenna which is separated by a distance d [36]:

$$P_r(d) = \frac{P_t G_t G_r \lambda^2}{4(\pi)^2 d^2} \qquad\qquad eqn.(3.0)$$

Where P_t is the transmitted power, $P_r(d)$ is the received power, G_t is the transmitter antenna gain, G_r is the receiver antenna gain, d is the Transmitter-Receiver separation distance in meters and λ is the wavelength in meters.

The Friis free space equation shows that the received power falls off as the square of the Transmitter-Receiver (T-R) separation distance. This implies that the received power decays at a rate of 20dB with distance.

The path loss, which constitutes signal reduction as a positive quantity measured in dB, is defined as the difference (in dB) between the effective transmitted power and the received power, and may or may not include the effect of antenna gains.

The path loss for the free space model when antenna gains are included is given by:

$$PL(dB) = 10 \log \frac{P_t}{P_r} \qquad \qquad \textbf{\textit{eqn. (3.1)}}$$

$$= -10 \log \left[\frac{G_t G_r \lambda^2}{4(\pi)^2 d^2} \right]$$

Eqn.(3.1) can be elaborated in terms of distance, d (km) and frequency, f (MHz):

$$PL(dB) = -10 \log_{10}(G_t) - 10 \log_{10}(G_r) - 20 \log_{10} \left[\frac{cx10^{-3}}{4\pi x f x 10^6} \right] - 20 \log_{10}(1/d)$$

$$= -G_t(dB) - G_r(dB) + 32.44 + 20 \log_{10}(d/km) + 20 \log_{10}(f/MHz)$$

3.2.2 Extended Coast-231 Hata Model

This model depends upon four parameters: frequency, height of a received antenna, height of a base station and distance from the base station to the received antenna.

The urban model eqn. is given by:

$$L(urban)(dB) =$$

$$46.33 + 33.9 \log f_c - 13.82 \log h_{tx} - a(h_{rx}) + (44.9 - 6.55 \log h_{tx}) \log d \qquad eqn. (3.2)$$

Suburban model eqn. is given by:

$$L(dB) = L(urban) - 2 \left[\log(f_c/28)\right]^2 - 5.4$$

Where $a(h_{rx})$ is

$$a(h_{rx}) = (1.1 \log f_c - 0.7)h_{rx} - (1.56 \log f_c - 0.8)dB \qquad eqn. (3.3)$$

3.2.3 Stanford University Interim (SUI)

The SUI outdoor path loss model is the reference propagation model for WiMAX system evaluation [38] and as such that will be the used model for the System Level Simulation (SLS). The model uses up to 6GHz frequency band. SUI can be used in three different terrains, Type A, B and C. The total attenuation $PL_{sui}(d)$ is given by:

$$20 \log_{10}(\frac{4\pi d_0}{\lambda}) + 10\gamma \log_{10}\left(\frac{d}{d_0}\right) + X_f + X_h + S \qquad eqn. (3.4)$$

where:

S is a zero-mean random Gaussian variable with standard deviation which represents the shadowing effect and it depends on terrain category.

d is the distance between transmitter and receiver;

d_0 represents the intercept distance and it is the maximum distance from the base stations for which the free space loss is valid.

λ is the wavelength;

γ represents the path loss exponent;

X_f is the frequency correction term;

X_h is the user antenna height correction term.

The path loss exponent γ depends on terrain category and on the base station height and it is equal to:

$$\gamma = a - b.h_b + \frac{c}{h_b}$$

Where **a, b, c** are constants for each terrain category as shown in Table3.1

h_b is the height of base station antenna ($10 < h_b < 80$ m).

Terrain A can be used for mountainous areas with moderate or very dense vegetation. This terrain presents the highest path loss, and it is considered as a dense populated urban area. Terrain B is characterized for the craggy terrains with rare vegetation, or flat terrains with moderate or heavy tree densities. This is the intermediate path loss scheme. This model is considered for suburban environment. Terrain C is suitable for flat terrains or rural with light vegetation, here path loss is minimum.

Table 3.1 Terrain category and Model parameter.

Model parameters	Terrain category		
	Type A	Type B	Type C
d_o	100m	100m	100m
A	4,6	4.0	3.6
B	0.0075m^{-1}	0.0065 m^{-1}	0.0050 m^{-1}
C	12.6m	17.1m	20.0m
σ_s	10.6Db	9.6dB	8.2dB

The frequency correction term X_f depends on the carrier frequency f and it is equal to:

$$X_f = 6.\log_{10}(\frac{f}{2000})$$

The user antenna height correction term X_h will depend on user antenna height h_r (2< h_r<10 m)

and on the terrain category and it is equal to:

$$X_h = \left(-10.8.\log_{10}(\frac{h_r}{2})\right) \text{ Type A and B}$$

$$X_h = \left(-20.\log_{10}(\frac{h_r}{2})\right) \text{ Type C .}$$

3.3 Coverage Estimation

In the coverage modeling, a system which employs Adaptive Modulation and Coding (AMC) is considered. The network has different physical layers $(i=1...N)$, where the first physical layer $(i=1,$ BPSK for WiMAX) is the most robust one and the last physical layer $(i=N,$ 64 QAM 3/4) is the most spectral efficient one. The probability of using a certain physical layer i, if it is the only one, in a cell with a radius R as shown in Figure 3.1 below is given by [39]:

Figure 3.1: Single cell scheme with a 3 sectors sector.

$$P_i = \frac{2}{R^2} \int_0^R p\left(P_r(x) > P_{s,i}\right).x\,dx \qquad\qquad eqn.\,(3.5)$$

Where $P_r(x)$ is the received power and $P_{s,i}$ is the threshold received power of the physical layer i.

For a system employing Adaptive Modulation and Coding the effective utilization of a physical layer i is given by the difference between the probability of using that physical layer and the probability of using the less robust one $(i+1)$. The received power $P_r(x)$ is given by the following relationship [40]:

$$P_{rx} = P_{tx} + G_{tx} + G_{rx} - PL \qquad\qquad eqn.\,(3.6)$$

31

P_{rx} is the power received and G_{rx} is the receiver's antenna gain in the direction of the transmitter. Here, the P_L term includes all attenuation due to path loss. Equation 3.6 describes the aggregate gain and attenuation of many competing signals. It also assumes that the radio link is isolated from any sources of external noise in the environment (i.e., thermal noise and interference from other transmitters). Commonly, the signal quality at a given point is written as the ratio between Signal and Noise: $SNR = P_{rx} - N$. alternately, if interference from a known set of interferers is included, the Signal to Interference and Noise Ratio (SINR) is defined as [41]:

$$SINR = P_{rx} - \left(N + \sum_{j}^{n} I_j \right) \qquad eqn. (3.7)$$

For a given real design and modulation scheme, there is a known relationship between Signal to Noise Ratio (SNR) and bit error rate. Using this relationship, we can determine the minimum detectable signal for a given radio as a function of the acceptable error rate: P_e, where P_e is the probability of bit error. Then, determining the points that are covered is simply the set of receiver locations that satisfy the inequality [41]:

$$P_{tx} + G_{tx} + G_{rx} - PL \geq MDS(P_e) \qquad eqn. (3.8)$$

Because the P and G terms are known for a network under evaluation, the coverage simulation becomes predicting the quantity PL given what is known about the environment, the distribution of CPEs and the radio link.

3.4 Shannon's Theory

This is define as the maximum transmission rate for a channel with bandwidth *B*, transmitted signal power *P* and noise spectrum *No* based on the notion that the channel is white Gaussian.

$$C = B \log_2(1 + \frac{P}{N0B}).$$ *eqn. (3.9)*

This is a SISO situation (single input, single output) and Eqn. 3.9 gives an upper limit for the attained error free SISO transmission rate. If the transmission rate is less than *C* bits/sec (bps), then a suitable coding scheme exists. To the contrary, if the transmission rate is more than *C* bps, then the received signal, irrespective of the robustness of the working code, it will contain errors.

3.5 Extended Capacity Formula for MIMO Channels

Vector channels, or multiple-input multiple-output (MIMO) channels, represent a very general description for a wide range of applications. They incorporate SISO (Single-Input Single-Output), MISO (Multiple-Input Single-Output) and SIMO (Single-Input Multiple-Output) channels as special cases. Often, MIMO channels are only associated with multiple antenna systems. However, they are not restricted to this case but can be used in a much broader context, for example, for any kind of multiuser communication. Principally, single-user and multiuser communications are distinguished. In the single user case, the multiple inputs and outputs of a vector channel may correspond to different transmit and receive antennas, carrier frequencies, or time slots due to the fact that the data stems from a single user [42].

In the basic MIMO concept, the data to be transmitted is scrambled, encoded, and interleaved and then divided up into parallel data flows, each of which modulates a separate transmitter.

Multiple antennas then capture the different streams, which have slightly different phases because they have travelled different routes, and combine them back into one.

Each multipath route can be treated as a separate channel, and the separate antennas take advantage of this to transfer more data. In addition to multiplying throughput, range is increased due to the advantage of antenna diversity, since each receive antenna has a measurement of each transmitted data stream.

The maximum data rate per channel grows linearly with the number of different data streams that are transmitted in the same channel, providing scalability and a more reliable link. This robustness allows the system to scale back the current to achieve the required data rate with minimal power consumption.

The modulation is orthogonal frequency division multiplexing (OFDM) using binary phase-shift keying (BPSK), quadrature phase-shift keying (QPSK), 16-phase quadrature amplitude modulation (16QAM), or 64QAM, depending on the data rate.

The multiple signals arrive at the receivers at different times in different phases, depending on the different paths they take. Some signals will be direct, others via multiple different paths. With this special multiplexing, each signal is unique as defined by the characteristics of the path it takes.

The unique signatures produced by each signal over the multiple paths allow the receivers to sort out the individual signals using algorithms implemented by DSP techniques. The same signals from different antennas then can be combined to reinforce one another, improving signal-to-noise ratio and, therefore, the reliability and range.

Perhaps the greater benefit of MIMO is the transmission's increased range and robustness, as it permits multiple streams. It also helps improve the signal-to-noise ratio and reliability significantly over other implementations.

Many MIMO systems use two transmitters and receivers, but the various standards allow other versions using different numbers of transmitters and receivers. Other possibilities include 2 by 3 (transmitters and receivers respectively), 3 by 2, 3 by 3, 3 by 4, 4 by 3, and 4 by 4. Beyond the 4-by-4 configuration, very little additional gain is normally achieved. The use of two transmitters and three receivers seems to be the most popular, although chipsets are now being implemented to support 4x4 MIMO for the highest-data-rate links.

Transmitting two or more data streams in the same bandwidth multiplies the data rate by the number of streams used.

With this channel bonding and four streams running on MIMO, a maximum potential data rate of 600 Mb/s is achievable. Data rates surpassing 100 Mb/s then can be supported over a 100-m range in hostile RF environments. [49]
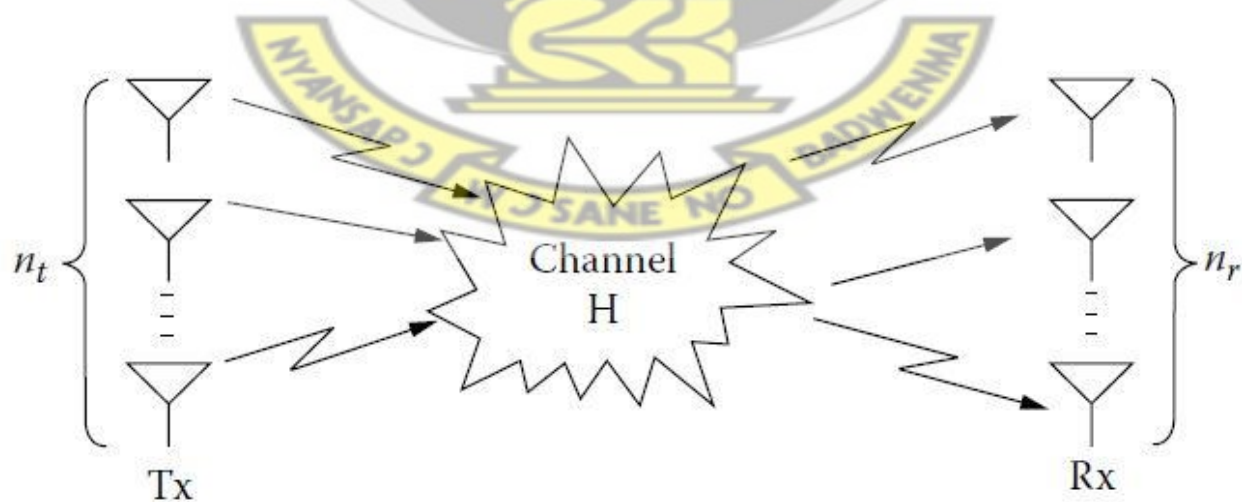

Figure 3.2 The MIMO channel.

For both multiple antennas at the transmitting and the receiving ends (Fig. 3.2), the channel displays multiple inputs and multiple outputs and its capacity can be assessed by the extended Shannon's theory, as accounted above.

3.5.1 General Capacity Formula

An antenna array with n_t at the transmitter and an antenna array with n_r elements at the receiver ends are considered. $h_{i,j}(\tau, t)$ is the impulse response between jth transmitter and the ith receiver. The multiple inputs and multiple outputs channel can be defined by the $n_r \times n_t$ $H(\tau, t)$ matrix:

$$\mathbf{H}(\tau, t) = \begin{bmatrix} h_{1,1}(\tau, t) & h_{1,2}(\tau, t) & \cdots & h_{1,n_t}(\tau, t) \\ h_{2,1}(\tau, t) & h_{2,2}(\tau, t) & \cdots & h_{2,n_t}(\tau, t) \\ \vdots & \vdots & \ddots & \vdots \\ h_{n_r,1}(\tau, t) & h_{n_r,2}(\tau, t) & \cdots & h_{M_R,n_t}(\tau, t) \end{bmatrix}$$

eqn. (3.10)

This matrix elements relate to the attenuation and phase shift that the wireless channel brings in during transmission with delay τ. This multiple inputs and multiple outputs system can now be explicit by eqn:

$$\boldsymbol{y}(t) = \mathbf{H}(\tau, t) \otimes \boldsymbol{s}(t) + \boldsymbol{u}(t) \qquad \textit{eqn. (3.11)}$$

Where $\otimes$ is convolution, $\boldsymbol{s}$(t) is $n_t \times 1$ vector equating to the n_t transmitted signals, $\boldsymbol{y}$(t) is $n_r \times 1$ vector equating to the n_r received signals and $\boldsymbol{u}$(t) is the additive white noise.

We assume the transmitted bandwidth is narrow enough that the channel response can be

handled as flat across frequency, then the discrete-time description corresponding to Eqn. 3.11

$$\mathbf{r}_\tau = \mathbf{H}\mathbf{s}_\tau + \mathbf{u}_\tau \qquad\qquad eqn.\ (3.12)$$

The capacity of a multiple inputs and multiple outputs channel was proved in [42, 43] can be estimated by the eqn.

$$C = \max \log_2[\det(\mathbf{I} + \mathbf{H}\mathbf{R}_{ss}\mathbf{H}^H)] \qquad\qquad eqn.\ (3.13)$$

$$tr(\mathbf{R}_{ss}) \le p$$

$\mathbf{H}$ is $n_r \times n_t$ channel matrix, $\mathbf{R}_{ss}$ is covariance matrix of the transmitted vector $\mathbf{s}$, $\mathbf{H}^H$ is the transpose conjugate of the $\mathbf{H}$ matrix and $\mathbf{p}$ is transmitting power. Eqn. 3.13 is the outcome of extended theoretical calculations, and its practical use is not obvious. Nevertheless, we can do linear shifts at both the transmitting and receiving end by converting the multiple inputs and multiple outputs channel to $n = min(n_r, n_t)$ which is SISO sub-channels and, hence, get more perceptive outcome. These shifts can be seen in [42].

3.5.2 Transformation of the MIMO Channel into n SISO Sub-channels

All channel matrix $\mathbf{H} \in \mathbb{C}^{n_r \times n_t}$ can be broke up according to its singular values. Suppose that for the aforementioned channel matrix this transformation is given by.

$$\mathbf{H} = \mathbf{U}\mathbf{D}\mathbf{V}^H \qquad\qquad eqn.\ (3.14)$$

where the matrices $\mathbf{U}$, $\mathbf{V}$ are unitaries of dimensions $n_r \times n_r$ and $n_t \times n_t$ accordingly, while $\mathbf{D}$ is a non-negative diagonal matrix of dimensions $n_r \times n_t$.

The diagonal elements of matrix $\mathbf{D}$ are the singular values of the channel matrix $\mathbf{H}$. The algorithm of singular value decomposition that provides the above transformation can be found in [44].

The operations that lead to the linear transformation of the channel into $n = min(n_r, n_t)$ **SISO**

sub-channels are described as follows: First, the transmitter multiplies the signal to be transmitted $\mathbf{x}_\tau$ with the matrix $\mathbf{V}$, the receiver multiplies the received signal $\mathbf{r}_\tau$ and noise with the conjugate transpose of the matrix $\mathbf{U}$. The above are presented in Equation 3.15 through Equation 3.17

$$\mathbf{S}_\tau = \mathbf{V}.\mathbf{x}_\tau \qquad \textit{eqn. (3.15)}$$

$$\mathbf{y}_\tau = \mathbf{U}^H.\mathbf{r}_\tau \qquad \textit{eqn. (3.16)}$$

$$\mathbf{n}_\tau = \mathbf{U}^H.\mathbf{u}_\tau \qquad \textit{eqn. (3.17)}$$

Substituting Equation 3.12 into Equation 3.16 gives:

$$\mathbf{y}_\tau = \mathbf{U}^H.\mathbf{r}_\tau \Rightarrow$$

$$\mathbf{y}_\tau = \mathbf{U}^H\mathbf{H}\mathbf{s}_\tau + \mathbf{U}^H\mathbf{u}_\tau \Rightarrow$$

$$\mathbf{y}_\tau = \mathbf{U}^H\mathbf{H}\mathbf{V}x_\tau + \mathbf{n}_\tau \Rightarrow$$

$$\mathbf{y}_\tau = \mathbf{U}^H\mathbf{U}\mathbf{D}\mathbf{V}^H\mathbf{V}\mathbf{x}_\tau + \mathbf{n}_\tau$$

Since $\mathbf{U}$ and $\mathbf{V}$ are unitary matrices, they satisfy $\mathbf{U}^H\mathbf{U} = \mathbf{I}_{n_r}$, $\mathbf{V}^H\mathbf{V} = \mathbf{I}_{n_t}$ and hence:

$$\mathbf{y}_\tau = \mathbf{D}\mathbf{x}_\tau + \mathbf{n}_\tau \qquad \textit{eqn.(3.18)}$$

Each component of the received vector y_τ can be written as:

$$\mathbf{y}_\tau^k = \boldsymbol{\varepsilon}_\tau\mathbf{x}_\tau^k + \mathbf{n}_\tau^k \qquad \textit{eqn. (3.19)}$$

where $\boldsymbol{\varepsilon}_k$ are the singular values of matrix $\mathbf{H}$ according to the transformation that took place above. Equation 3.19 implies that the initial (n_r, n_t) MIMO system has been transformed into $n = min(n_r, n_t)$ SISO subchannels, as illustrated in Figure 3.3.
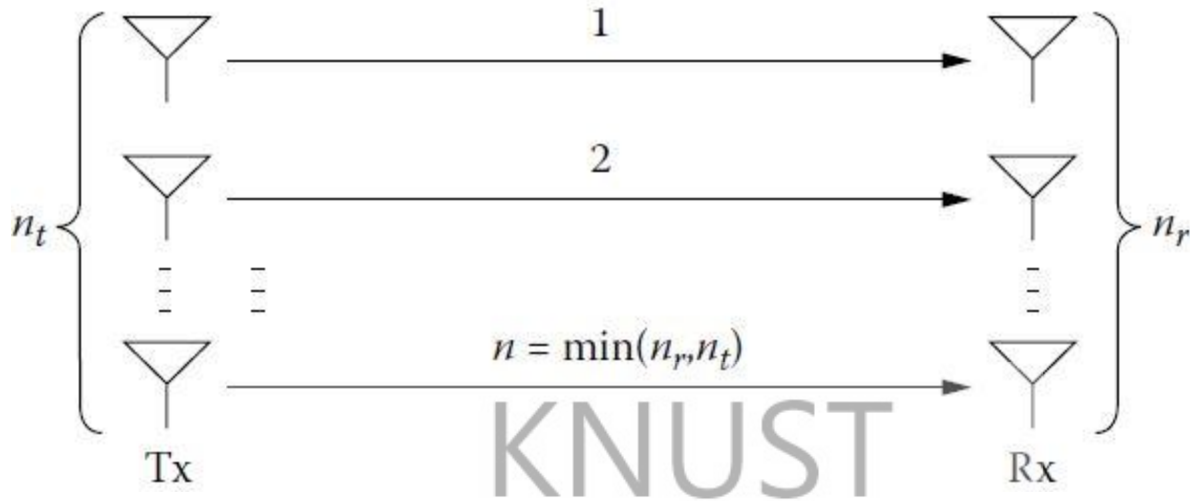
Figure 3.3 Conversion of the MIMO channel into n SISO sub-channels.

The above analysis of a Multiple Antenna Element (MEA) system capacity is presented in [42]. It was proven in [42] that the total capacity of n SISO Sub-channels is the sum of the individual capacities and as a result the total MIMO capacity is:

$$C = \sum_{k=1}^{n} \log_2 (1 + P_k \varepsilon_k^2) \qquad\qquad eqn.\,(3.20)$$

Where p_k is power allocated to the *kth* sub-channel and ε_k^2 is its power gain. We notice that according to the singular value decomposition algorithm ε_k^2 , k = 1, 2, …, n are the eigen values of the **HH**^{H} matrix, which are always non-negative. Furthermore, regardless of the power allocation algorithm used, p_k must satisfy

$$\sum_{k=1}^{n} p_k \leq P$$

because of the wanted power constraint.

At this point, there are two cases of particular interest that need further consideration: the knowledge (or not) by the transmitter of the Channel State Information (CSI). These are described in the next sections.

3.5.3 No CSI at the Transmitter

Considering Equation 3.20, we notice that the achieved capacity depends on the algorithm used for allocating power to each sub-channel. The theoretical analysis assumes the channel state known at the receiver. This assumption stands correct since the receiver usually performs tracking methods in order to obtain CSI, however the same consideration does not apply to the transmitter.

When the channel is not known at the transmitter, the transmitting signal s is chosen to be statistically non-preferential, which implies that the n_t components of the transmitted signal are independent and equi-powered at the transmit antennas. Hence, the power allocated to each of the n_t subchannels is $p_k = p/n_t$. Applying the last expression to Equation 3.17 gives:

$$C = \log_2[\det(\mathbf{I} + \frac{p}{n_t})\mathbf{H}\mathbf{H}^H]$$
eqn. (3.21)

OR

$$C = \sum_{k=1}^{n} \log_2(1 + \frac{p}{n_t}\varepsilon_K^2)$$
eqn. (3.22)

3.5.4 CSI at the Transmitter

In cases in which the transmitter has knowledge of the channel, it can perform optimum combining methods during the power allocation process. In that way, the SISO sub-channel that contributes to the information transfer the most is supplied with more power.

One method to calculate the optimum power allocation to the **n** sub-channels is to employ the water pouring algorithm (a detailed discussion of this algorithm can be found in [45]).

Considering the assumption of CSI at the transmitter, we can proceed to the following capacity formula.

$$C = \sum_{k=1}^{n} \log_2\left(1 + \frac{\gamma_k \cdot p}{n_t} \varepsilon_k^2\right) \qquad \qquad \boldsymbol{eqn.\,(3.23)}$$

The difference between Equation 3.22 and Equation 3.23 is the coefficient γ_k that corresponds to the amount of power that is assigned to the kth sub-channel. This coefficient is given by:

$$\gamma_k = E\{|s_k|^2\} \qquad \qquad \boldsymbol{eqn.\,(3.24)}$$

and satisfy the constraint

$$\sum_{k=1}^{n} \gamma_{k=n_t}$$

The goal with the water pouring algorithm is to find the optimum γ_k that maximizes the capacity given in Eqn. 3.23.

3.5.5 Channel Estimation at the Transmitter

As mentioned earlier, the CSI is not usually available at the transmitter. In order for the transmitter to obtain the CSI, two basic methods are used: the first is based on feedback and the second on the reciprocity principle.

In the first method the forward channel is calculated by the receiver and information is sent back to the transmitter through the reverse channel. This method does not function properly if the channel is changing fast. In that case, in order for the transmitter to get the right CSI, more frequent estimation and feedback are needed. As a result, the overhead for the reverse channel becomes prohibitive. According to the reciprocity principle, the forward and reverse channels are identical when the time, frequency and antenna locations are the same. Based on this principle the transmitter may use the CSI obtained by the reverse link for the forward link. The main problem with this method emerges when frequency duplex schemes are employed.

3.6 Bounds on MIMO Capacity

The lower and upper bounds of MIMO capacity were first derived in [42]. Four basic assumptions are considered in this work and summarized here for simplicity.

• The transmitter has no previous knowledge of the channel.

• The parallel sub-channels produced by the decomposition of the MIMO channel are independent.

• The wireless channel is submitted to Rayleigh fading.

• The transmitter antenna array elements are less than the receiver's antenna elements $(n_t < n_r)$.

In addition, we cite four mathematical expressions that will be used for deriving the wanted capacity bounds [42].

$$\det(\mathbf{DD}^H + \mathbf{RR}^H) \geq \prod_{\ell}(|\mathbf{D}_{\ell,\ell}|^2 + |\mathbf{R}_{\ell,\ell}|^2) \qquad\qquad eqn.\,(3.25)$$

where matrices **D** and **R** are diagonal and upper-triangular, respectively.

$$\det(I + AB) = \det(I + BA) \qquad \textit{eqn. (3.25)}$$

$$\det(I + QAQ^H) = \det(I + A) \qquad \textit{eqn. (3.26)}$$

where A, B are square matrices and Q is a unitary matrix.

$$\det(x) \leq \prod_e x_{e,e} \qquad \textit{eqn. (3.27)}$$

KNUST

where x is a non-negative definite matrix.

Since the channel is submitted to Rayleigh fading, the channel matrix $\mathbf{H}$ is given by $\mathbf{H}_w$, which is referred to as spatially white matrix. The elements of $\mathbf{H}_w$ can be modeled as zero mean circularly symmetric complex Gaussian (**ZMCSCG**) random variables. The $\mathbf{H}_w$ has particular statistical properties that can be found in [45, 46]. We consider the transformation $\mathbf{H}_w = \mathbf{QR}$, where $\mathbf{Q}$ is a unitary and $\mathbf{R}$ is an upper-triangular matrix. This transformation is referred to as Householder Transformation [47]. According to this transformation the elements of $\mathbf{R}$ above the main diagonal are statistically independent, while the magnitude of the main diagonal entries are chi-squared distributed with $2n_r, 2(n_r - 2 + 1), \dots, 2(n_r - n_t + 1)$ degrees of freedom. Using Equation 3.21:

$$C = \log_2[\det(\mathbf{I} + \tfrac{p}{n_t}\mathbf{HH}^H)] = \log_2[\det\left(\mathbf{I} + \tfrac{p}{n_t}\mathbf{QRR}^H\mathbf{Q}^H\right)] \Rightarrow$$

$$C = \log_2[\det\left(\mathbf{I} + \tfrac{P}{n_t}\mathbf{RR}^H\right)] \geq \log_2[\prod_e(1 + \tfrac{p}{n_t}\left|R_{e,e}\right|^2)] \Rightarrow$$

$$C \leq \sum_{e=1}^{n_t} \log_2\left(1 + \frac{p}{n_t}\left|R_{e,e}\right|^2\right) \qquad \textit{eqn. (3.28)}$$

Equation 3.28 corresponds to the lower capacity bound and practically shows that this bound is

defined by the sum of the capacities of n_t independent subchannels with power gains that follow the chi-square distribution with $2n_t$, $2n_r - 2, ..., 2(n_t - n_t + 1)$ degrees of freedom. In order to find the upper bound of the capacity, Equation 2.23 is used again:

$$C \leq \sum_{e=1}^{n_t} \log_2 \left(1 + \frac{p}{n_t}\left(\left|R_{e,e}\right|^2 + \sum_{m=e+1}^{n_t} \left|R_{e,m}\right|^2\right)\right) \qquad eqn.\,(3.29)$$

The upper bound of the capacity is the sum of the capacities of n_t independent subchannels, with power gains chi-squared distributed and with degrees of freedom $2(n_r + n_t - 1), 2(n_r + n_t - 3), ..., 2(n_r - n_t + 1)$. The difference of the mean values of the upper and lower bounds is less than 1b/s/Hz.

3.7 Capacity of Orthogonal Channels

It is interesting to study the case where the capacity of the MIMO channel is maximized. We consider the simple case of $n_r = n_t = n$, along with a fixed total power transfer through the SISO subchannels (i.e., $\sum_{k=1}^{n} \varepsilon_k^2 = a$, where a is a constant). The capacity in Equation 3.22 is concave in the variables ε_k^2 (k= 1, 2, ..., n) and, as a result, it is maximized when $\varepsilon_k^2 = \varepsilon_i^2 = a = $ a/n, (k, i = 1, 2,..., n). The last equation reveals that the $\mathbf{HH}^H$ matrix has n equal eigenvalues. Hence, $\mathbf{H}$ must be an orthogonal matrix, i.e.,$\mathbf{HH}^H = \mathbf{H}^H\mathbf{H} = (\,a/n)\mathbf{I}_n$. Substituting $\mathbf{HH}^H = (\,a/n)\mathbf{I}_n$ into Equation 3.21:

$$C = \log_2\left[\det\left(\mathbf{I} + \frac{pa}{n^2}\mathbf{I}_n\right)\right] \Rightarrow C = n.\log_2(1 + \frac{pa}{n^2}) \qquad eqn.\,(3.30)$$

If $\|\mathbf{H}_{i,j}\|^2 = 1$, the matrix $\mathbf{H}$ satisfies $\mathbf{HH}^H = nI_n$, hence, Equation 3.21 becomes:

$$C = \log_2\left[\det\left(\mathbf{I} + \frac{P}{n}nI_n\right)\right] \Rightarrow C = n.\log_2(1 + p) \qquad eqn.\,(3.31)$$

The last Eqn. 3.31 indicates that the capacity of an orthogonal MIMO channel is n times the capacity of the SISO channel. The results of these models will be presented in Figure 4.2.

3.8 MIMO capacity estimation based on the deployed scenario

In order to effectively estimate the average user throughput, the system deployment in terms of Base Station placements, Sectorization and frequency reuse planning has to be taken into consideration. The number of users, placed throughout the cellular area, is considered and the effect of channel variations such as path loss and shadow fading are incorporated into the analysis. Frequency reuse scenarios may be described by denotation "N_c x N_s x N_f", where N_c is number of independent frequency channels in the WiMAX network, N_s is the number of sectors per cell and N_f is the number of segments in exploited frequency channel is used for the SLS. For example Figure 3.4 shows the WiMAX network deployment for 1x3x1 frequency reuse planning.
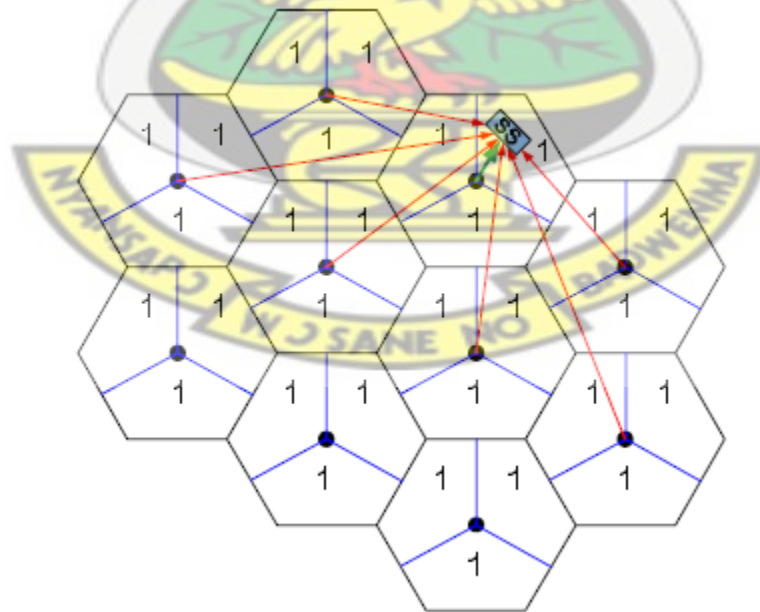

Figure 3.4 Deployment scenario

To obtain output metrics of mobile WiMAX system in interference-limited environment, a SLS methodology based on time-domain evolution to perform fast link adaptation in accordance with PHY abstraction model based on instantaneous channel capacity of realistic frequency selective link layer channel is used. This dynamic downlink methodology can be shortly described as follows. The CPEs are evenly distributed in the hexagon area with radius of $3R$. For each CPE, random shadow fading factors with specified correlation between BSs are generated. CPEs received powers from the BS taking into account attenuation factor including propagation path loss, generated shadowing, BS and target CPE antenna gains, angle loss (BS antenna pattern), cable loss, receiver noise, etc. For each CPE connected to the BS, the burst spanning 2 consecutive OFDMA symbols (1 PUSC symbol) and all loaded data subcarriers is transmitted. At each burst transmission, the independent ITU-R link level channel realizations are generated for serving BS and all interfering BSs. The post-processing signal-to-interference plus noise ratios (SINR) per subcarrier are calculated in accordance with specific signal processing technique provided by IEEE Standard 802.16e and exploited in current system configuration Calculated instantaneous post processing SINR values are inputs of PHY abstraction model that is used for prediction of instantaneous link performance. For each CPE that is served by the BS, the fast link adaptation process is repeated in conditions of time-varying frequency-selective home BS channel and interference levels.

For each target user, the throughput is evaluated on the base of instantaneous spectral efficiency values collected over all the Monte-Carlo trials. The equal time spectral efficiency is defined as the average data rate for all target subscribers normalized by the total bandwidth required for the deployment [48]:

$$SE^1 = k_F \left[\frac{1}{\dot{N}_{SS}} \sum_{i=1}^{\dot{N}_{SS}} SE_i \right] \cdot \left(\frac{N_s}{N_f} \right) \cdot K_{load} \qquad\qquad eqn.\,(\textbf{3.32})$$

$$SE^1 = k_F \cdot \left[\frac{1}{\dot{N}_{SS}} \frac{1}{N_{tr}} \sum_{i=1}^{\dot{N}_{SS}} \sum_{t=1}^{\dot{N}_{SS}} se_{i,t} \right] \cdot \left(\frac{N_s}{N_f} \right) \cdot K_{load}$$

where k_F is the ratio of number of data subcarriers to the total number of subcarriers (720/1024 for 10 MHz DL PUSC), $\acute{N}_{SS}$ is the number of target users served by the BS of the central cell for given shadow fading values, N_{tr} is number of trial snapshots with fixed shadow fading values, $se_{i,t}$ is the instantaneous spectral efficiency of the ith subscriber for t^{th} snapshot, SE_i is the averaged (across snapshots) spectral efficiency of the ith subscriber, K_{load} is the loading factor (the percentage of sub-channels allocated by the BS for the given sector or given cell).
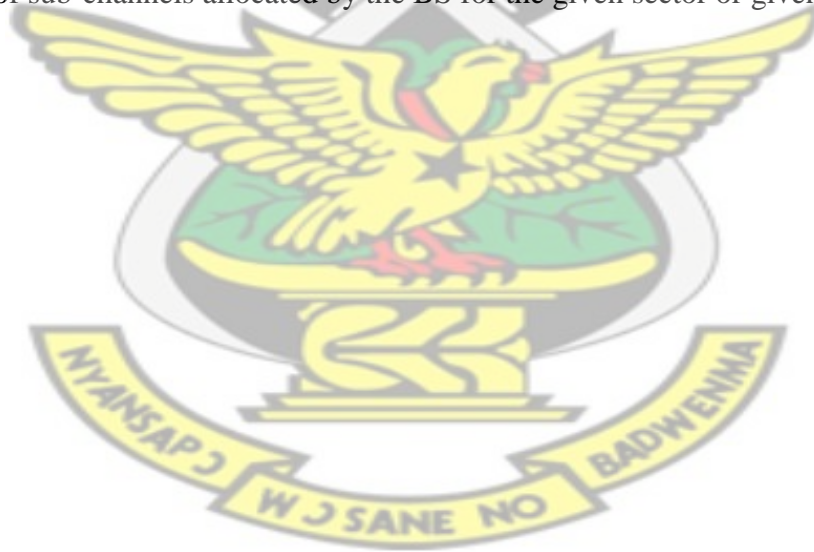
Chapter Four: System Implementation and Testing

4.1 Introduction

In this chapter, the results based on the approach used in Chapter Three are presented. The simulation model adopted for analyzing the capacity and coverage range of the deployed WiMAX network is based on the behavior of users and the distribution of CPEs in the cell. The simulation was done using the stochastic distribution of CPEs within the cell site as shown in Figure 4.0. Our model consists of a circular placement of nodes in a hexagon with one WiMAX Base Station and ten (10) Subscriber Stations (SS) which were 2.91km and 3.0km respectively apart from the Base Station (BS). These nodes are fixed and mobile nodes since mobility has been configured. The BS connected to the IP backbone via Vodafone Ghana's Fiber link.
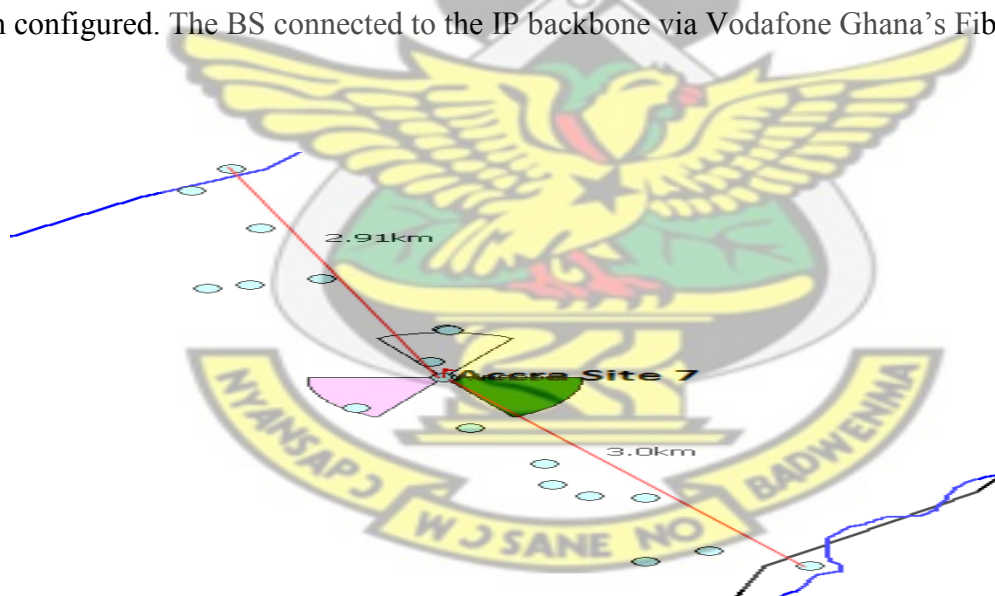

Figure 4.1 Dispersion of CPE around the base station

The simulation parameters are summarized in Table 4.1. Genex-Unet Modeler was used with matlab tool to facilitate the usage of in-built models of commercially available network elements, with reasonably accurate emulation of various real life network topologies.

Table 4.1 Simulation Parameters

Resource frequency	2.5-2.53GHz
Channel Bandwidth	10MHz
Frequency reuse scheme	FFR, PUSC
Average users per sector	10
Fast Fourier Transform (FFT) Size	1024
Subcarrier spacing	10.93 kHz
Useful symbol time	91.4μs
Guard time	11.4μs
OFDMA symbol time	102.8μs
Gain	18dBi
Horizontal Beamwidth (3dB)	60°
Vertical Beamwidth (3dB)	8°
Maximum power	43dBm
Antenna height	40m
CPE Antenna Config	2T2R
Height of CPE Antenna	2m

Different frequency reuse scenarios have been designed in our simulation with different FFR and PUSC schemes to measure the performance of some parameters such as throughput and network coverage. The coverage simulation of the site has also been done to help analyze the strength of the received power within the site. The capacity with different reuse factors and various Downlink/Uplink (TDD split) schemes have been simulated. The final site radio Link budget was done with Genex-Unet. Note that the channel bandwidth and subcarrier spacing are related as follows [48]:

Subcarrier spacing*FFT size = Channel Bandwidth * Sampling rate, for 10 MHz channel, with 28/25 sampling rate, and 1024 FFT, Subcarrier spacing = 10*(28/25)/1024 = 10.9375 kHz.

Table 4.0 shows that at 10MHz the OFDMA symbol time is 102.8 microseconds and so there are 48.6 symbols in a 5 millisecond frame only. These symbols will be used for the TDD DL/UL split ratios which will be used for the average throughput per sector simulation. Out of the 48.6 symbols, 1.6 symbols are used for Transmit-Transmit Gap and Receive-Transmit Gap leaving 47 symbols which will be split for the DL/UL ratios.

4.2 Discussion of Simulation Results

The capacity simulation of the WiMAX Base Station based on the simulation parameters is summarized in Figure 4.2 and Table 4.2. The results in Figure 4.2 shows the theoretical performance of the MIMO configuration whiles Table 4.2 show the practical performance of the MIMO configurations based on the network simulation parameters used at the site under consideration.

In Figure 4.2, With 10 MS, received antenna gain of the base station of $18dBi$ and with maximum transmitted power and equivalent radiated power of 18dBm and 21dBm respectively,

the bits per second performance for the 4*4 MIMO System for SNR value of $30dB$ is around 35

Mbps which overwhelms the practical simulation results as shown in Table 4.2.
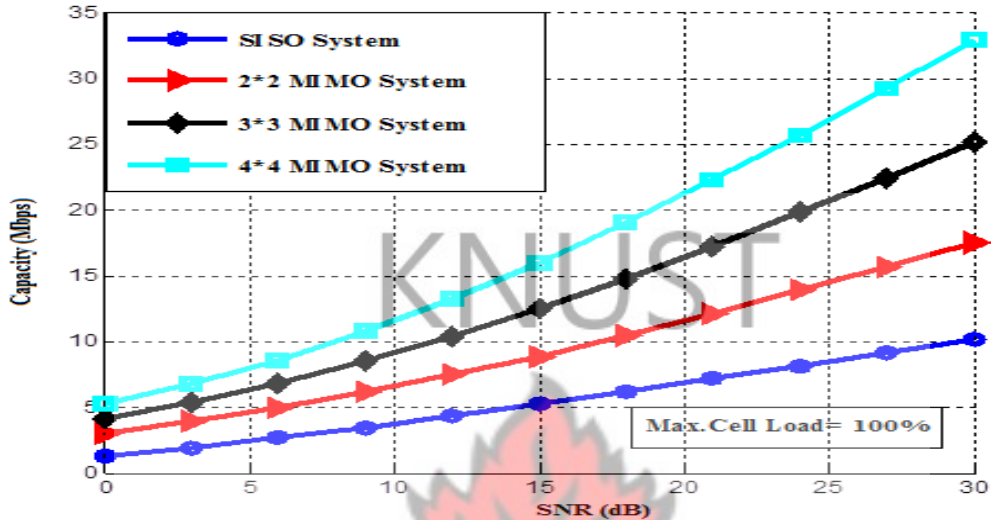

Figure 4.2 Open Loop simulation results

The result in Figure 4.2 is similar and complements the results obtained for the theoretical

performance of MIMO in outdoor environments in [50].

 From the results, it can be seen that it is possible to attain maximum data rate of 8.45Mbps using

adaptive 2x2 MIMO antenna configuration and a DL/UL ratio of 35:12. With the same

configuration when 4x4 adaptive MIMO configuration is used, the capacity improves to 8.82

Mbps. It is important to mention here that with the capacity analysis only path loss, receiver

noise figured, implementation loss and number of transmitting antennas are considered, link

margin receiver sensitivity, noise floor and channel matrix are excluded.

Table 4.2 Opened loop throughput simulation results

| Bandwidth	Permutation	TDD Split Ratio	WiMAX Carrier Average Throughput per sector			
			2T2R Adaptive MIMO(Mbps)		4T4R adaptive MIMO(Mbps)	
			DL	UL	DL	UL
10 MHz	PUSC with all SC 1x3x3	26:21	5.73	2.18	5.99	2.76
	PUSC with all SC 1x3x3	29:18	6.64	1.81	6.93	2.30
	PUSC with all SC 1x3x3	31:15	7.24	1.45	7.56	1.84
	PUSC with all SC 1x3x3	35:12	8.45	1.09	8.82	1.38
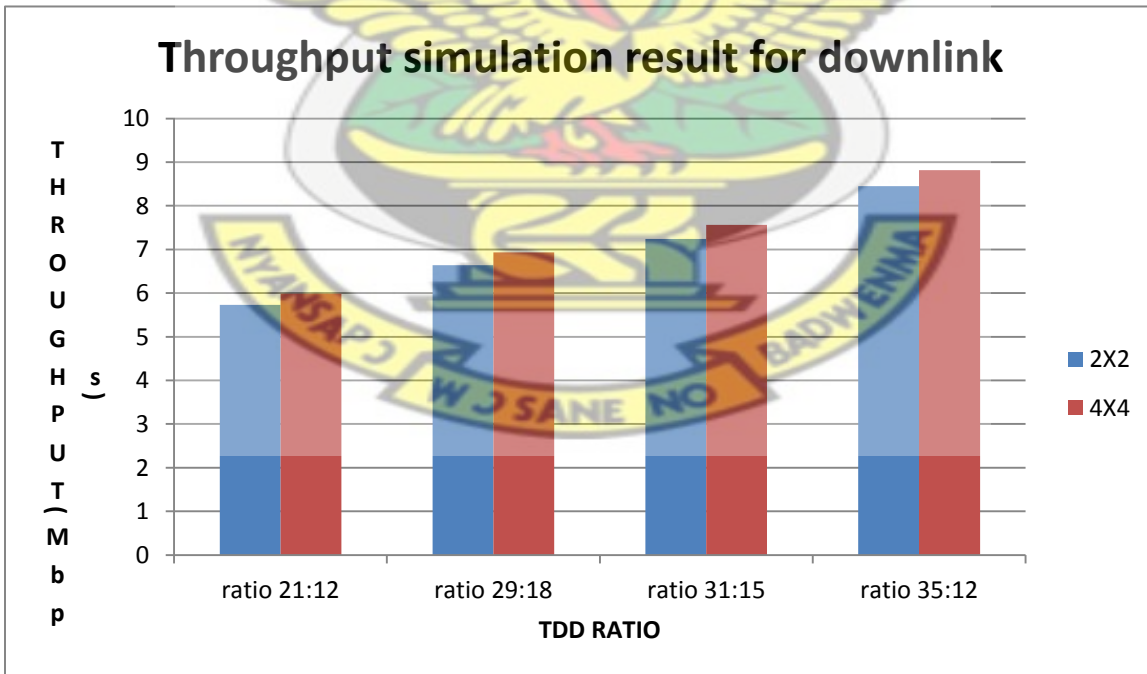
Figure 4.3 Throughput simulation result for downlink from Table 4.2

Path loss simulation using SUI with Multiuser Detection (MUD) at a cell range of 1.357 km was around $110.67 dB$. It was also realized that as the cell range and allowable path loss in dB decreases, the cell load increases dramatically. Interestingly, similar results were obtained in [16] where they further observed that base station multiuser detection (MUD) receiver can provide good coverage even with high system load after initial deployment and, finally, concluded that the effect of MUD on cell range depends on propagation environment. It worth noting that the performance of the of the 3x3 MIMO configuration is just below that of 4x4, hence, it could be used when the 4x4 is not available because for signal to noise ratio of 30dB, it is possible to achieve a capacity of 25 Mbps. The capacity performance for SISO as well as the 2x2 system is not encouraging as for SNR of 30dB the capacity is 10 Mbps and 17 Mbps respectively.

The link budget for the network site under study is done using Genex-Unet. The final radio (link budget) is simulated using equations (3.6)-(3.8).

The link budget for the area under study is shown below.
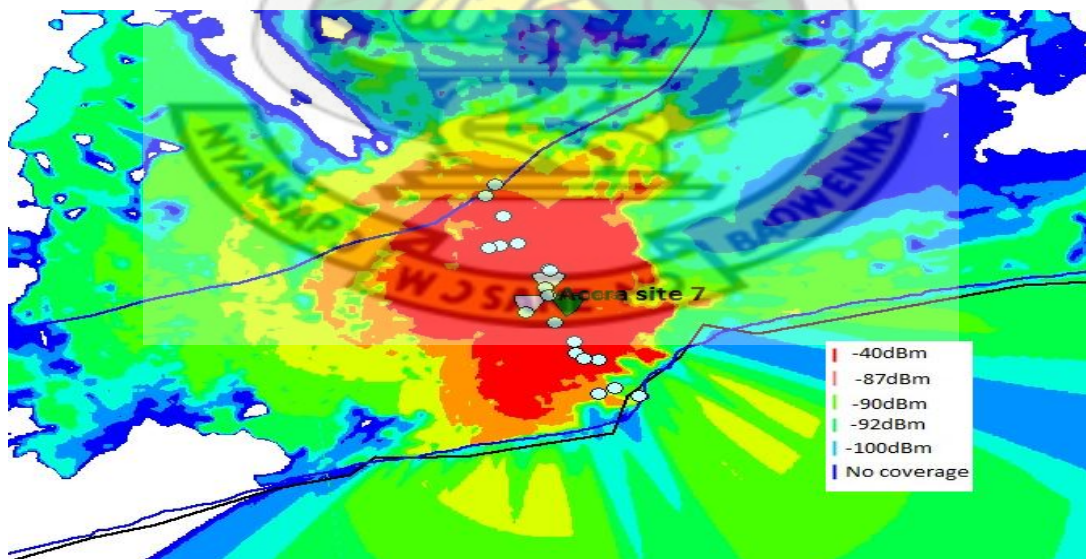
Figure 4.4 Radio network simulations

53

The simulated center RSS of -40dBm was obtained at a modulation scheme of 64-QAM up to about 620m away from the base station. The simulated cell edge RSS value was -92dBm at a modulation scheme of QPSK at a distance of about 4km away from the BS.

4.3 Real field trial measurements

The main objective of this research is to make a performance comparison between simulation results and field experimental data. In order to achieve that objective, the performance evaluation of a WiMAX network deployed in the urban center of Accra has been done. The distance and coverage testing is one of the most significant tests which has been done, since this test is of very high importance to subscribers in the study area. The measurement setup comprises.

1.   GPS

2.   Dongle XCAL-X

3.   Laptop with a XCAL-X software

4.   Van
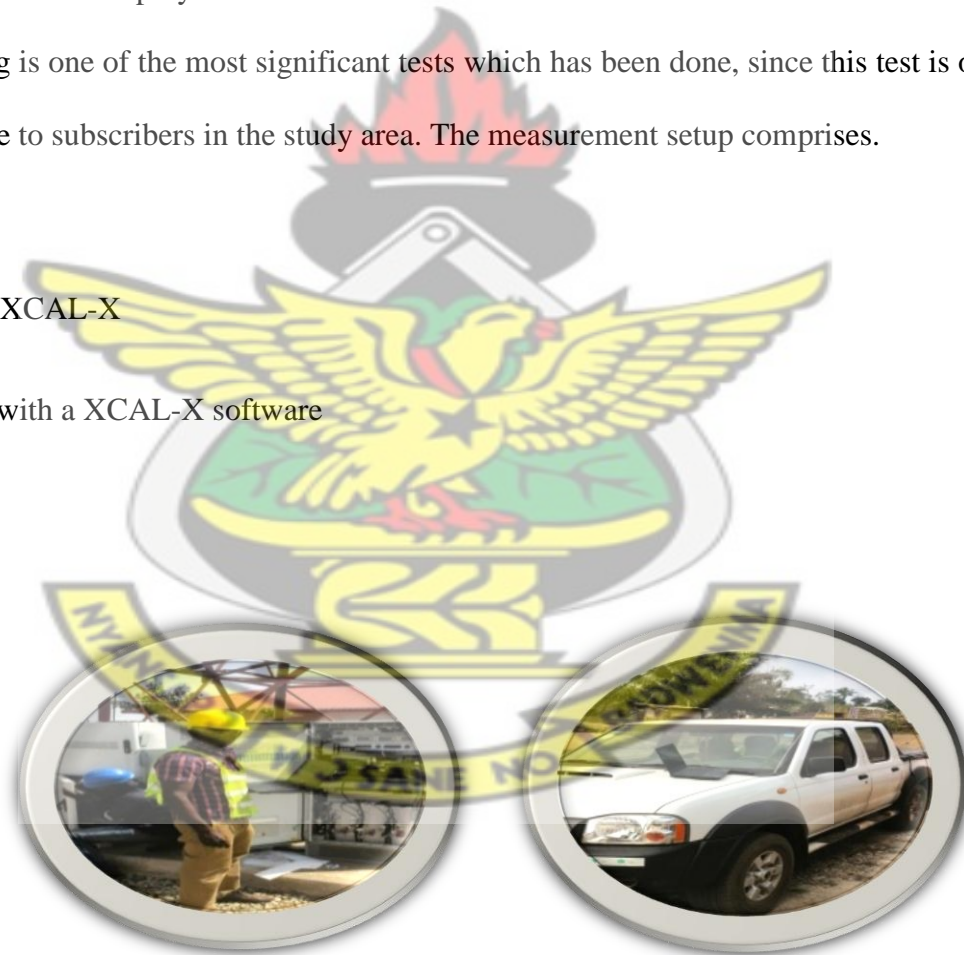
Figure 4.5 WiMax Test-Bed Setup

The QPSK modulation scheme was chosen to maximize the network coverage. In order to increase the subscriber unit's distance from the base station and measure the link quality and throughput performance for all locations, the downlink/uplink ratio of 26:21 was chosen to balance the downlink and the uplink throughput, while the other parameters remained the same.

4.4 Field Measurements Summary

The field measurement was carried around the University of Ghana Campus. This area provides a measure of the WiMAX network's radio distance in a typical urban area. This particular location was chosen because of its representative nature of urban complications in deploying outdoor wireless networks. Most areas within the measurement areas are fairly obstructed, with a few segments surrounded by dense foliage. There are high buildings in the vicinity of the test road in this area.

4.4.1 Coverage

The Received Signal Strength (RSS) and Carrier to Interference plus Noise ratio (CINR) were done in over 16,000 locations within the cell site.

The measured RSS and CINR values were mapped with the GPS information of the area with the color path showing the amount of measured RSS as shown in Figure 4.6. The highest RSS value of -45dBm was measured at a distance of 500m away from the base station as compared with the simulated value of -40dBm. The measured cell edge RSS value was -100dBm at about 4km away from the BS. The summary of the RSS measurement is shown in Figure 4.7.
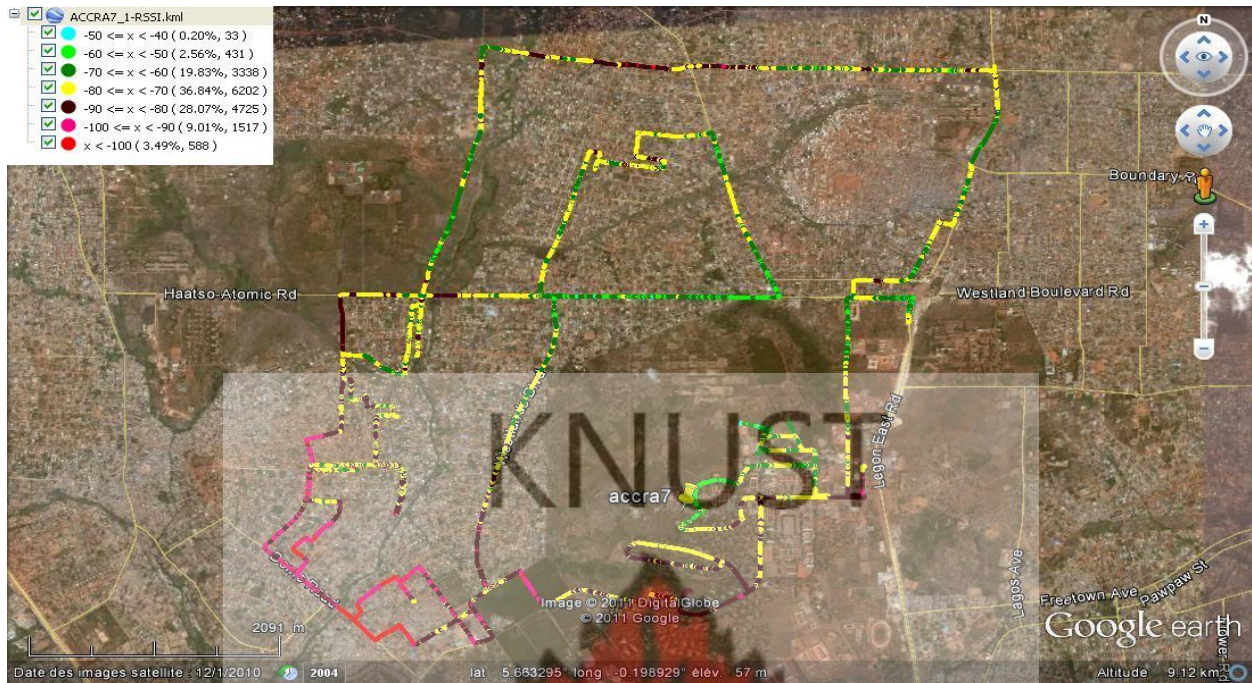
**Figure 4.6 Locations of RSS measurement within the BS**
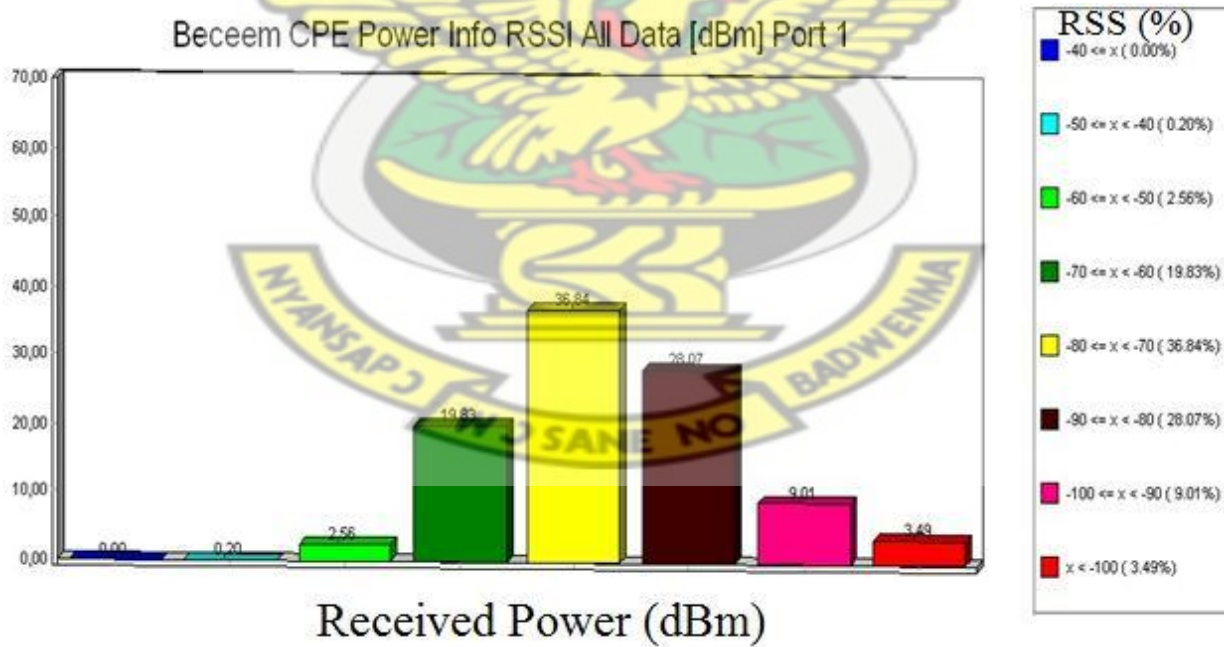
Figure 4.7 Summary of RSS measurements within the BS

The CINR values measured between the base station and the mobile client are shown in Figure 4.8 and 4.9. The highest measured CINR of 35 dB was measured at a modulation of 64-QAM. This value was measured from the BS to a distance of 500m at 876 locations along the route.
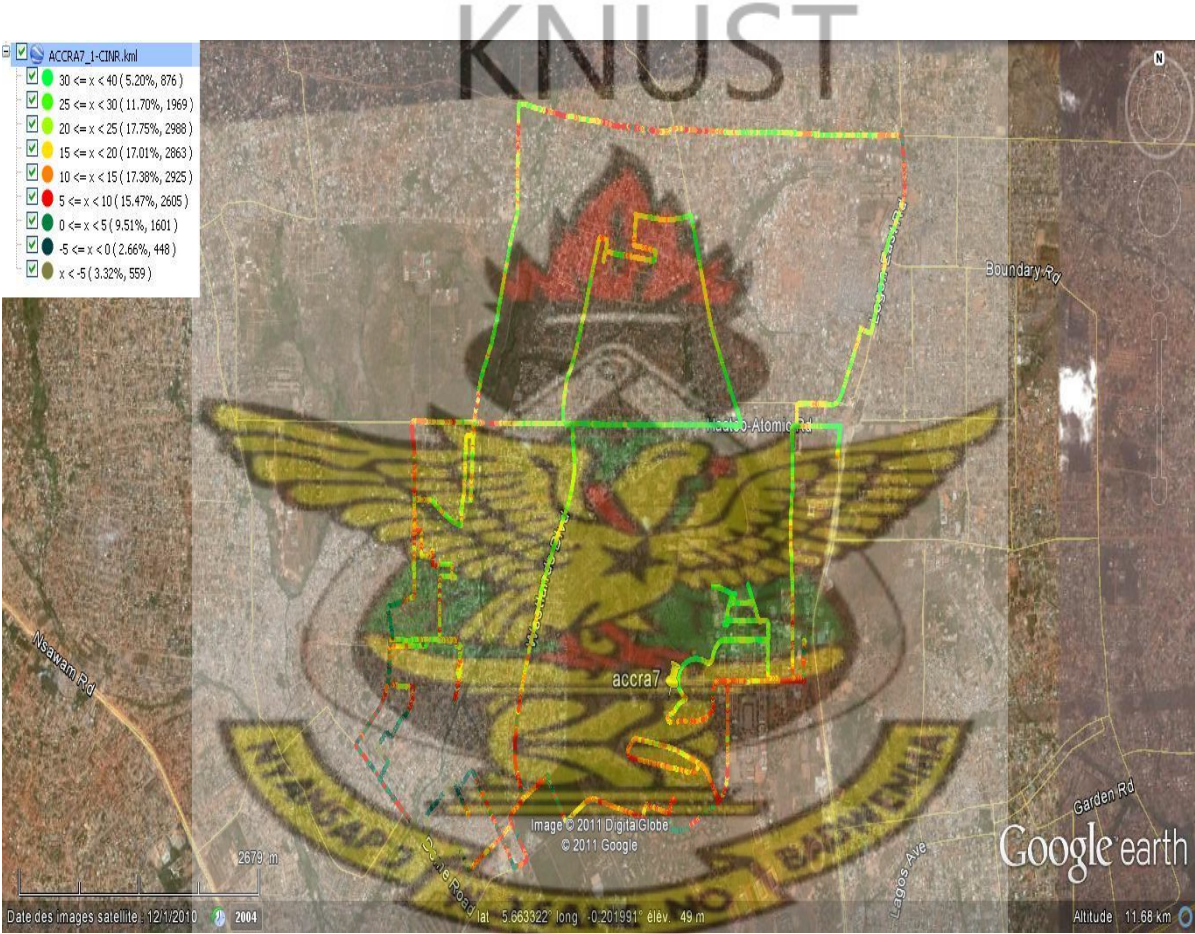

Figure 4.8 Location of CINR measurements within the BS

The CINR measurement with respect to the measured distances is summarized in Figure 4.10. These parameter measurements will form the basis for modeling the critical CINR.
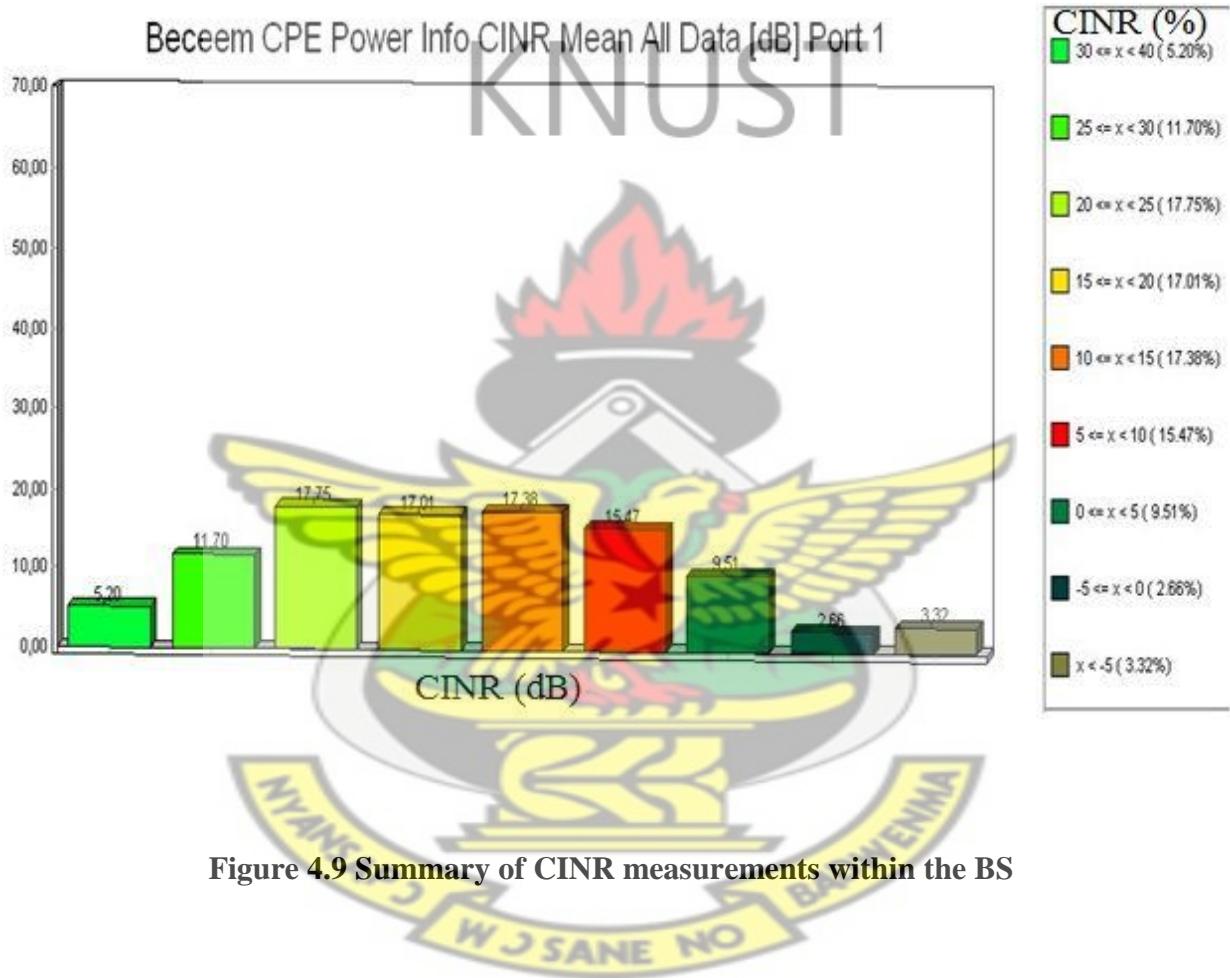
Figure 4.9 Summary of CINR measurements within the BS

The summary of the Field trial measurement data results is shown in Appendix A.
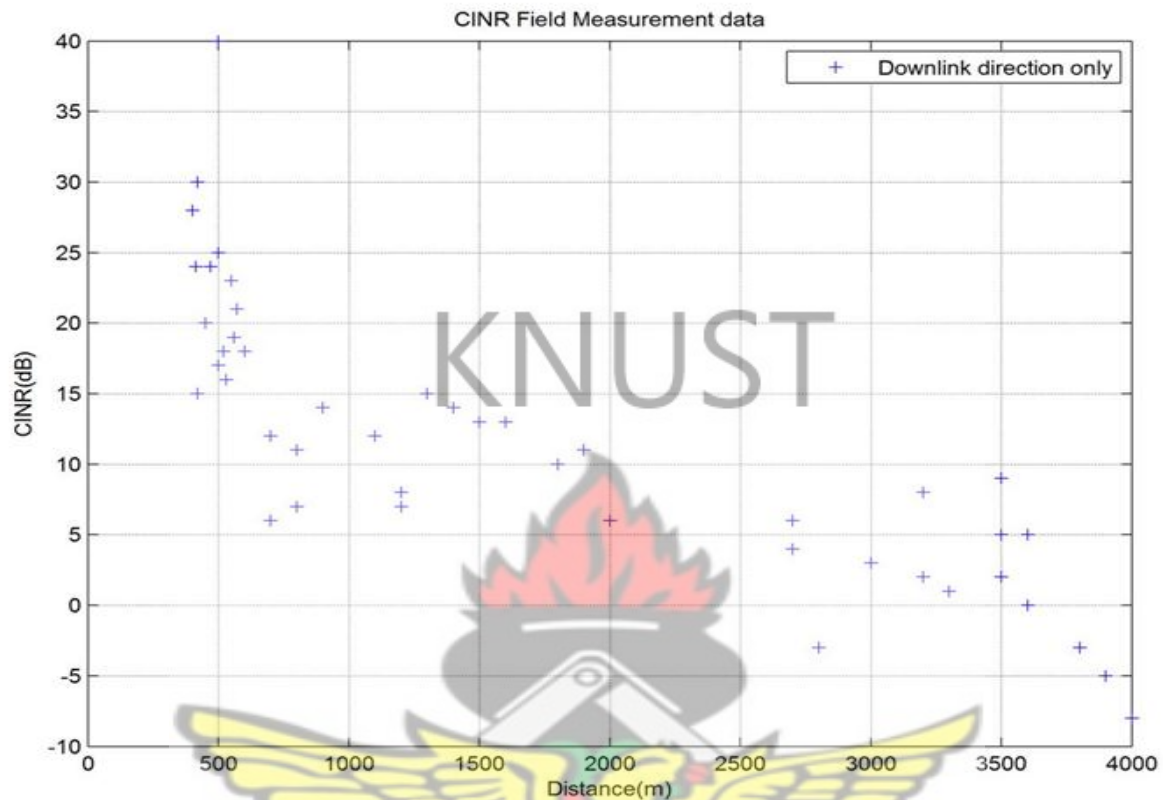

Figure 4.10 Summary of CINR measurements

About 79.29 % of the measured CINR values were between 25dB to 5dB. The least measured value of -6dB was obtained at a modulation of QPSK at a distance of 4km before connection was dropped.

4.4.2 Throughput Performance

The subsequent tests focused on the network's throughput performance. 20Mb FTP packet traffic was transmitted from the Base station to the subscriber unit, which was located in the drive test Van. The Base station's transmit power was set to 30dBm. At the beginning of throughput test, the Van was close to the Base station, and then moved away along drive test route. After the subscriber unit was out of communication range and lost the connection, the van was turned around and moved back towards the location of the Base station. The Van was kept at a steady velocity of 60 mph during the test. Figure 4.11 summarizes the throughput measurement and illustrates the downlink and uplink throughput measurement within the site with respect to CINR. The maximum measured DL and UL throughput values of 6.10Mbps and 2.08Mbps respectively were obtained at a distance of 400m away from the BS.
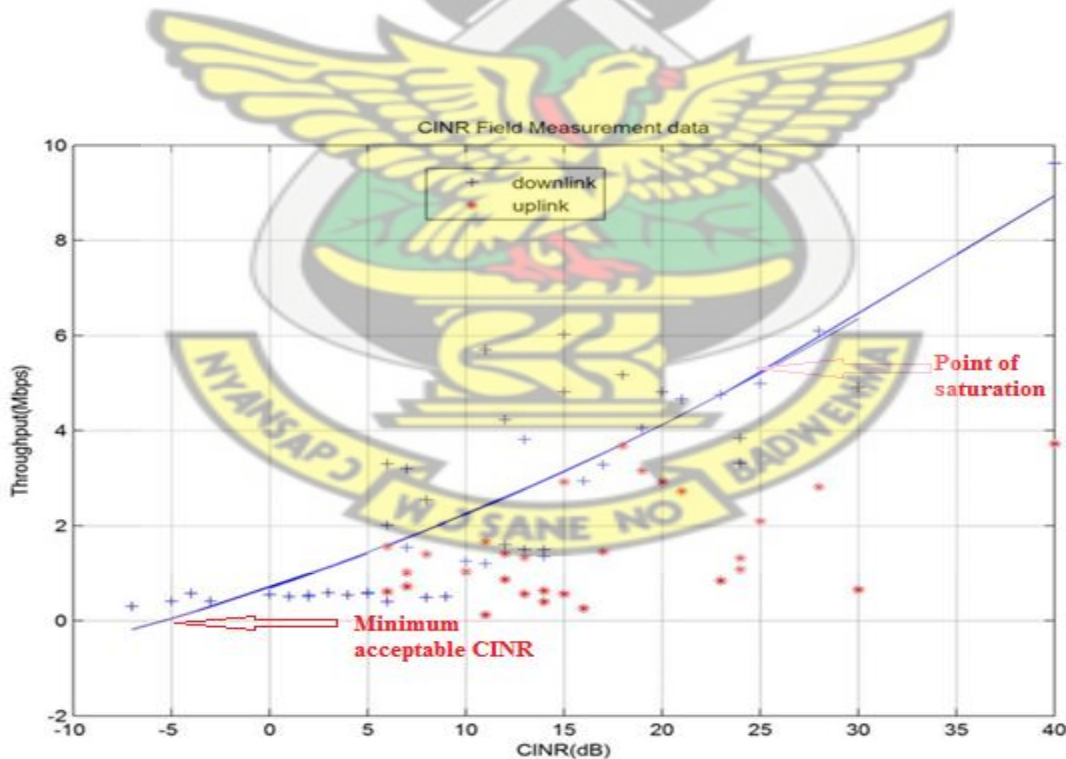

Figure 4.11 Summary of throughput measurement within the site

It was observed that, the downlink performance was quite stable at 5.6 Mbps within the range of 500m to 1.5km as shown in Figure 4.11.
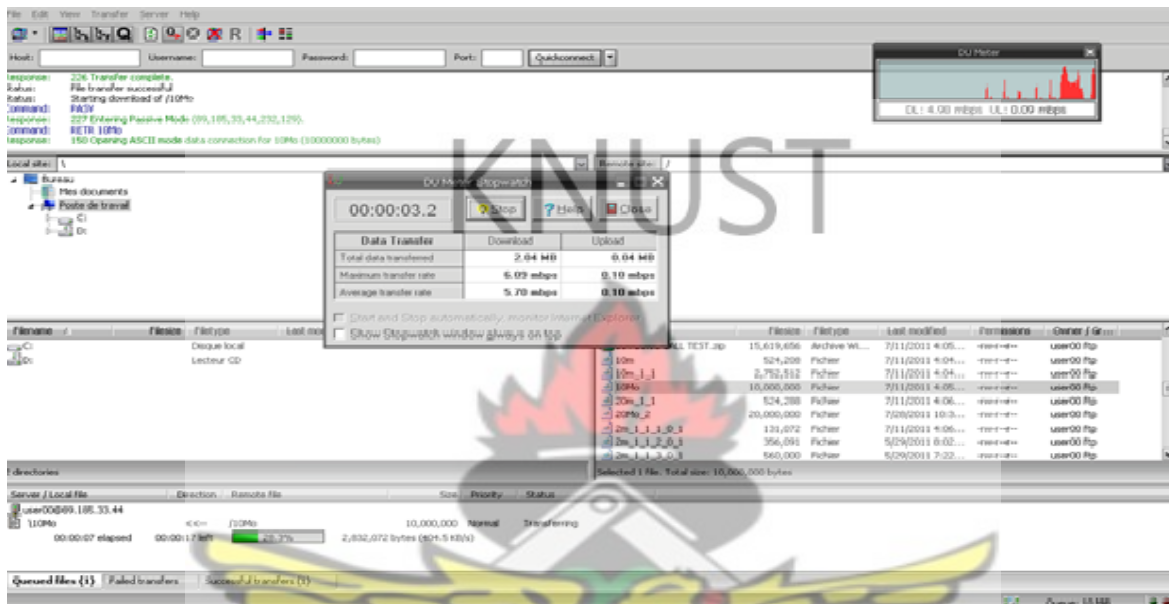
Figure 4.12 Snapshot of throughput measurement

The least measured DL and UL throughput of 300kbps and 156kbps respectively were measured at a distance of about 4km away from the BS.

From the field measurement results, the RSS value of -100dBm was measured at a distance of 4km at a modulation scheme of QPSK as against the simulated distance of 5km. This measured distance is adequate to provide ubiquitous coverage to all the CPEs in the service area. From the US Federal Communication Commission's broadband speed guide and similar work done in [15-19] in Europe and United states, the measured cell edge DL throughput of 300kbps is adequate to support standard video conferencing applications, hence, the network performance of the deployed network is adequate enough to serve its intended purpose.

Analysis of coverage of the network conducted in this research has revealed that the propagation environment affects the cell range with a given cell loading.

4.5 Comparison between the simulated and the field measured results
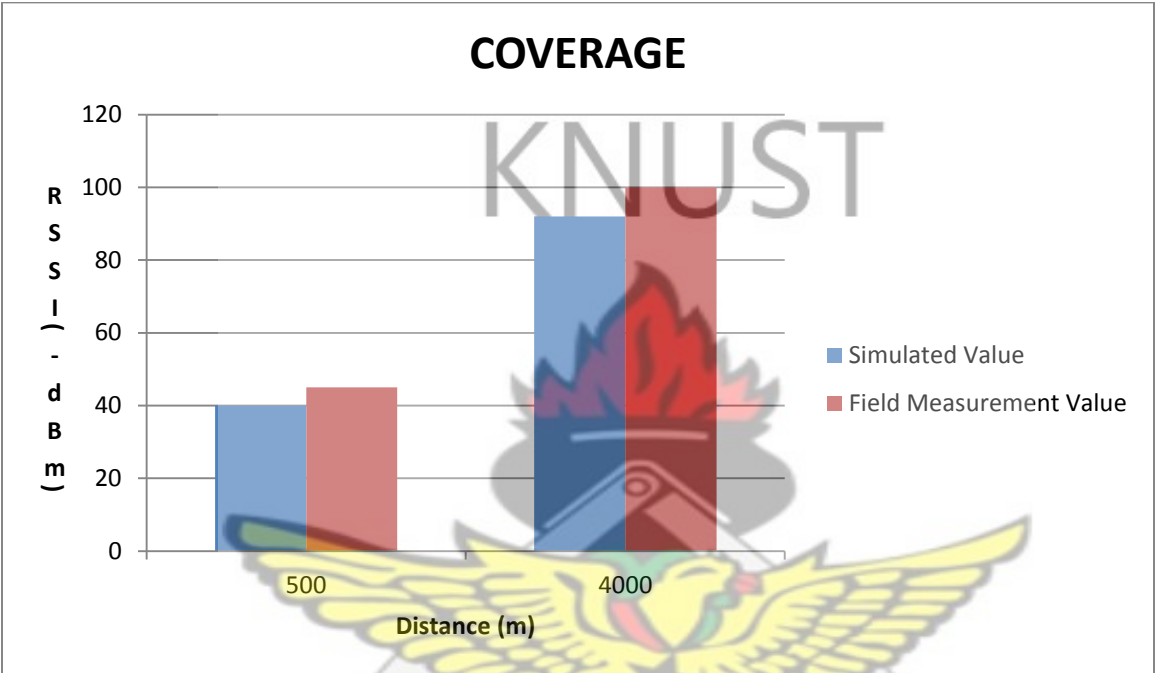
Figure 4.13 Coverage comparison

The stimulated results shows a maximum RSSI value of -40dBm at a distance of 500 meters close to the BS as compare to field measured value of -45dBm at the best modulation scheme of 64QAM and minimum simulated RSSI value of -92dBm at a distance of 4km as against -100dBm at robust modulation scheme QPSK at the cell edge as shown in figure 4.13 above.
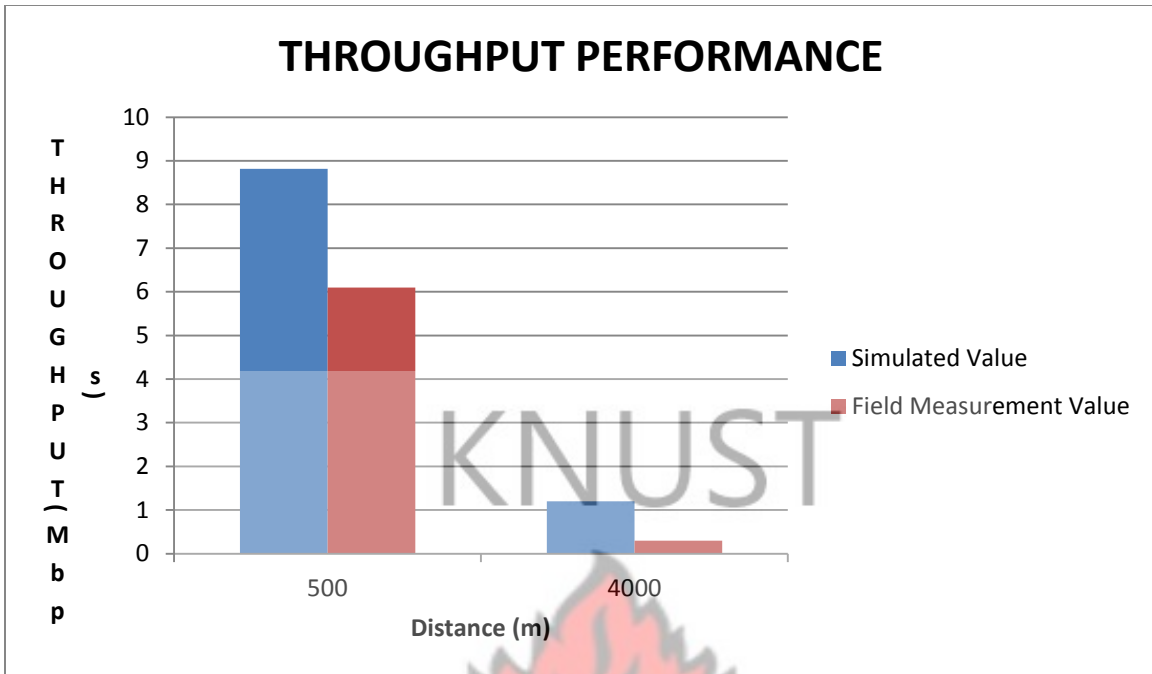
Figure 4.14 Throughput comparison

From figure 4.14, the maximum field measured downlink throughput is 6.1Mbps as compare to the stimulated downlink throughput value of 8.82Mbps and at the cell edges the minimum simulated value is 1.2Mbps as against field measured value of 300Kbps.
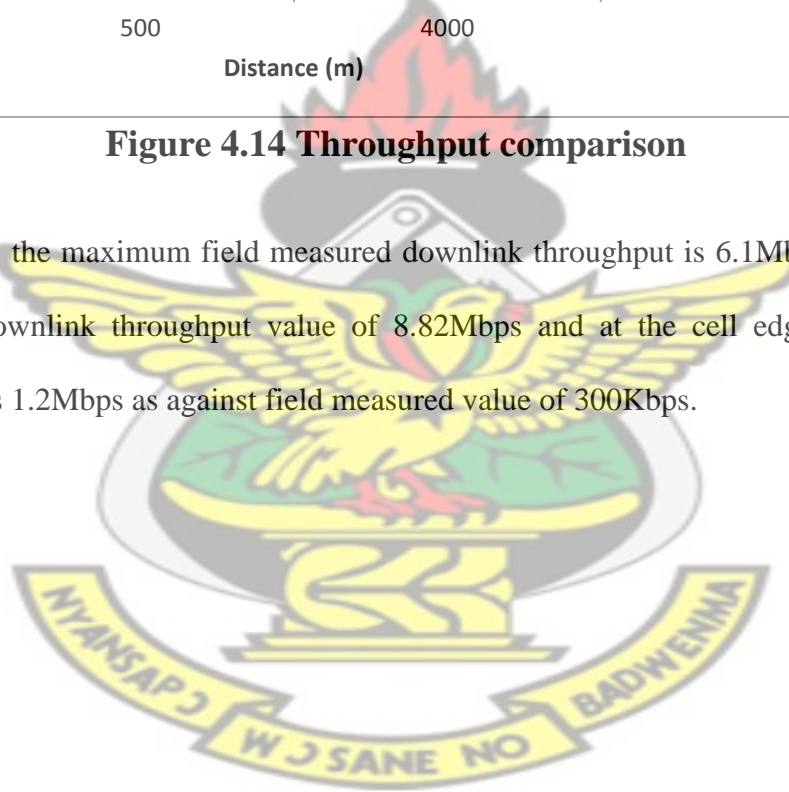
Chapter Five: Conclusion and Recommendation

5.1 Conclusion

Even in its first generation, WiMAX is showing 2-3 times performance over today's 3G (HSPA). With the next iteration of the standard, 802.16m, WiMAX will evolve and offer even greater speeds, just as LTE is coming to the Ghanaian market. Both WiMAX and LTE have many similarities and both require significant upgrades to existing network equipment and phones – the evolution path from a 3G to 4G network is very similar regardless of an operator's choice of 4G technology.

This thesis uses a dynamic system level simulation methodology of WiMAX system to do a comparison between simulated and field measured values. The performance characteristics of the WiMAX network that allow evaluating capabilities of this technology in realistic multi cell deployment scenarios are obtained for single-input single output and multiple antenna configurations. Deployment of mobile WiMAX network with 1x3x3 frequency planning using 2x2 MIMO system configurations has been found to be an acceptable way for network providers to mitigate interference. From the evaluation, it has been found that from up to 1.5km from the BS, the network performance was very good with average measured throughput of 5.6Mbps and can support any broadband application.

From the analysis of field measured results, the greatest advantage of the deployed WiMAX BS over existing mobile broadband systems is the high throughput measured over longer distances.

From the evaluation, it can be seen that the WiMAX networks can serve the insatiable demand for wireless broadband services in Ghana.

5.2 Recommendations for Future Study

In Ghana, the major competitor to WiMAX network is 3G systems. Currently, NITA and DiscoveryTel are the only Operators to have successfully deployed WiMAX systems. Most mobile broadband service providers have remained focused on current 3G services and are not taking part in WiMAX tests or deployments. NITA besides the deployment of a WiMAX network has made moves to deploy 3GPP-LTE on pilot basis in Accra.

WiMAX and LTE are convergence upon 4G technology that includes seamless handover, QoS, security, and higher-level compatibility such as user authentication and billing across yet dissimilar low-level interface networks.

As Mobile WiMAX is a new standard and not many certified products are available in the market nor many trials and deployments are performed under the African conditions, it is a topic that has huge research potential. Many experts believe that the future *4G* platform will be formed as a combination of LTE and WiMAX standards. So the most controversy would be upon the global market share for each of these mobile broadband technologies. Therefore, each of these innovative service providers will compete to include the state-of the art technologies in their supporting standard as soon as they appear. Coexistence study between WiMAX and LTE deployment in Ghana is recommended.

More recent releases of Mobile WiMAX will implement a substantial number of innovative technologies such as; SIMO, MIMO, AAS and beam forming. Employment of each of these techniques can affect the capacity by increasing the total throughput and resource efficiency, via

different signaling procedure. On the other hand, new amendment such as higher velocity support is an example of applications that will restrict the system's actual throughput.

Therefore, upgrading the measurement parameters to include more BS than discussed in this thesis based on these additional features can be looked as an interesting future work.

In conclusion, developing a user friendly planning tool by exploring the capacity calculations and propagation and coverage modeling that covers the overall network considerations over a city wide carrying out would be a great area of interest to researchers.

REFERENCES

[1] David Turahi. WSIS the Way Forward, Online:www.kus.uu.se/pdf/publications/ICT/Post-WSIS Dr Turahi, [Accessed on 27/02/2013].

[2] Xuemin Huang and Jijun Luo: Automatic Configuration and Optimization of WiMAX Networks, published in WiMAX Network Planning and Optimization Yan ZhangISBN: 978-1-4200-6662-3.

[3] Mehlfuhrer, S.Caban, S., and Rupp, M. (2008) Experimental Evaluation of Adaptive Modulation and Coding in MIMO WiMAX with Limited Feedback, EURASIP Journal on Wireless Communications and Networking, Vol. 2008: pp. 1-12.

[4] Ghana- Telecoms, mobile, broadband and forecast: A buddecom report, 11th edition page 44. Accessed online: http://www.budde.com.au/Research/Sample-Reports.aspx 1st Jan, 2013.

[5] IEEE 802.16 Working Group, "IEEE Standard for Local and Metropolitan Area Networks–Part 16: Air Interface for Fixed Broadband Wireless Access Systems," IEEE Std. 802.16-2004, October 2004.

[6] IEEE Std 802.16e-2005, "IEEE Standard for Local and metropolitan area networks--Part 16: Air Interface for Fixed Broadband Wireless Access Systems--Amendment 2: Physical and Medium Access Control Layers for Combined Fixed and Mobile Operation in Licensed Bands," Feb. 2006.

[7] Jeffrey, G., Arunabha , G., and Rias, M. (2007) Fundamentals of WiMAX: Understanding Broadband Wireless Networking , New York : Prentice-Hall.

[8] GSM World, "Market data summary." http://www.gsmworld.com/newsroom/market-data/market_data_summary.htm.

[9] 3GPP, "Technical specification group services and system aspects; release 1999 specifications 3G TS 21.101 version 1.0.0," Oct. 1999.http://www.3gpp.org/ftp/Specs/html-info/21101.htm.

[10] T. Halonen, J. Romero, and J. Melero, GSM, GPRS and EDGE Performance: Evolution Towards 3G/UMTS, 2nd ed. John Wiley and Sons Ltd, 2003.

[11] W.Webb and R. Steele, "Variable rate QAM for mobile radio," IEEE Transactions on Communications, vol. 43, no. 7, pp. 2223–2230, July 1995, doi: 10.1109/26.392965.

[12] M. Lee et al., "Emerging Standards for Wireless Mesh Technology," IEEE Wireless Commun., vol.13, no. 2, Apr. 2006, pp. 56–63.

[13] WiMAX End-to-End Network Systems Architecture - Stage 2: Architecture Tenets, Reference Model and Reference Points," WiMAX Forum, December, 2005.

[14] K.Majewski,U. Tuerke,X.Huang, and B.Bonk,Analytical cell load assessment in OFDM radio networks, in Proceedings of the 18th Annual IEEE International Symposium on Personal, Indoor and Mobile Radio Communications (PIMRC"07), Athens, Greece, 2007.

[15] Grøndalen,O., Grønsund,P.,Breivik,T., Engelstad.P, "Fixed WiMAX Field Trial Measurements and Analyses", Mobile Summit 2007, Budapest (Hungary), July 1-5, 2007.

[16] C. Eklund, R-B. Marks, S. Ponnuswamy, K-L.Stanwood, and N-V. Waes, "WirelessMAN Inside the IEEE 802.16 Standard for Wireless Metropolitan Networks," IEEE Standards Information Network/IEEE Press, May 2006, pp. 400.

[17] Manal Al-bzoor and Khaled Elleithy: WiMAX basics from PHY layer to scheduling and multicasting approaches [online, accessed 18/8/2013].

[18] Jeffrey De Bruyne, Wout Joseph, LeenVerloock and Luc Martens: Measurement and Evaluation of a network performance of a fixed WIMAX system in suburban environments, [online, accessed 18/8/2013].

[19] Mardeni.R, Siva Priya.T: "Performance of Path Loss Model in 4G Wimax Wireless Communication System in 2390 MHz", 2011 International Conference on Computer Communication and ManagementProc .of CSIT vol.5 (2011) IACSIT Press, Singapore.

[20] K.Majewski,U. Tuerke,X.Huang, and B.Bonk, Analytical cell load assessment in OFDMradio networks, in Proceedings of the 18th Annual IEEE International Symposium on Personal, Indoor and Mobile Radio Communications (PIMRC"07), Athens, Greece, 2007.].

[21] Xuemin Huang and Jijun Luo: Automatic Configuration and Optimization of WiMAX Networks, published in WiMAX Network Planning and Optimization Yan ZhangISBN: 978-1-4200-6662-3.

[22] WIMAX Forum: WiMAX System Evaluation Methodology, V2.1 Created on July 7, 2008.

[23] T. Wang, H.H Refai: Empirical Network performance Analysis on IEEE 802.11 with different Protocols and signal to Noise Ratio Values, in international conference on wireless and optical communications Networks (WOCN 2005), Dubai. United Arab Emirates, March 2005, pp. 29-33.

[24] Azizul H. , M. (2007) Performance Evaluation of WiMAX/IEEE 802.16 OFDM Physical Layer , M.S. Thesis , Helsinki university of Technology, Espoo, Finland.

[25] Y. Leiba, Y. Segal, Z. Hadad, and I. Kitroser, "Coverage/ Capacity simulations for OFDMA PHY in with ITU-T channel model," IEEE C802.16d-03/78, Nov. 2004, pp.24.

[26] Rama Rao, T. VijayaBhaskara Rao, S. Prasad, M.V.S.N. MangalSain, Iqbal, A. and Lakshmi, D. R. 2000. Mobile Radio Propagation Path Loss Studies at VHF/UHF Bands in Southern India. IEEE Transactions On Broadcasting, 46(2), pp. 158-164.

[27] Tapan, K. S. Zhong, J. Kyungjung, K. Abdellatif, M. and Magdalena Salazar-Palma 2003.A Survey of Various Propagation Models for Mobile Communication. IEEE Antennas and Propagation Magazine, 45 (3), No.3.

[28]COST 231 Final Report 1999. Digital Mobile Radio: COST 231 View on the Evolution Towards 3rd Generation Systems, Commission of the European Communities and COST Telecommunications, Brussels.

[29] Perez-Vega, C. and Zamanillo, J.M. 2002. Path Loss Model for Broadcasting Applications and Outdoor Communication Systems in the VHF and UHF Bands. IEEE Transactions On Broadcasting, 48(2), pp. 91-96.

[30] Hata, M. Empirical formula for propagation loss in land mobile radio services. IEEE Trans. Veh. Technol., 29(no issue number), pp. 317–325.

[31] Lee, W.C.Y. Estimation of local average power of a mobile radio signal. IEEE Trans.Veh. Technol., 34(1), pp. 22–27.

[32] Ikegami, F. Yoshida, S. Takeuchi, T. and Umehira, M. 1984. Propagation factors controlling mean field strength on urban streets. IEEE Trans. Ant. Prop., vol. 32 (no issue number), pp. 822–829.

[33] Walfisch, J. Bertoni, H. L. 1988. A Theoretical Model of UHF Propagation in Urban Environments. IEEE Transactions On Antennas And Propagation, 36(12), pp. 1788-1796.

[34] ITU Geneva 1989. Final Acts of the Regional Administrative Conference for the Planning of VHF/UHF Television Broadcasting in the African Broadcasting Area and Neighbouring Countries.

[35] Armoogum V., Mohamudally N, Propagation Models and their Applications in Digital Television Broadcast Network Design and Implementation, Trends in Telecommunication Technologies, 2012, pp 165-184.

[36] Friis, H.T. 1946.The Free Space Transmission equation. Proc. IRE, vol. 34, p.254.

Gaudrel, R. Betend, C. 1997. DIGITAL TV BROADCAST Field Trials on the Experimental NetworkofRennes,Internal VALIDATE documentfromCCETT, FT.CNET/DMR/DDH.

[37] Kozono, S. Watanabe, K. 1977. Influence of Environmental buidings on UHF Land mobile radio propagation, IEEE Trans. Commun., 25(10), pp.1133-1143.

[38] H. Yaghoobi, "Scalable OFDMA Physical Layer in IEEE 802.16 WirelessMAN,"Intel Technology J., vol. 8, no. 3, pp. 202-212, Aug. 2004.

[39] CDMA2000 Evaluation Methodology," 3GPP2 .P1002-C-0, September 2004.

[40] WiMAX Forum, "WiMAX System Evaluation Methodology V2.1," July 2008, 230 pp. Available:http://www.wimaxforum.org/resources/documents/technical.

[41] C. So-In, R. Jain, and A. Al-Tamimi, "AWG Analytical Model for Application Capacity Planning over WiMAX V0.8," WiMAX Forum,Application Working Group (AWG) Contribution, Sept. 2009. Available:http://www.cse.wustl.edu/jain/papers/capmodel.xls.

[42] D.S. Shiu, J. Foschini, J. Gans, and J.M Kahn. 2000. "Fading correlation and its effect on the capacity of multi element antenna system," IEEE Transactions on Communications, 48, 502, 2000.

[43] I.E. Telatar, "Capacity of multi-antenna Gaussian channels," Eur. Trans. Telecom., Vol. 10, No. 6, Dec. 1999.

[44] Online: http://www.cs.ut.ee/~toomas_1/linalg/lin2/node14.html [accessed on 14/06/2014].

[45] A. Paulraj, R. Nabar, and D. Gore. 2003. Introduction to Space-Time Wireless Communications, Cambridge: Cambridge University Press, Chap. 4.

[46] G.J. Foschini. 1996. "Layered space-time architecture for wireless communications in a fading environment when using multi-element antennas," Bell Labs Tech. J., Autumn 1996, pp. 41–59.

[47] Online: http://rkb.home.cern.ch/rkb/AN16pp/node123.html [accessed on 4/09/2014].

[48] IEEE document 802.11-04-172r1 "The "Black-Box" PHY Abstraction Methodology," (Atheros, Mitsubishi).

[49] Online:http://electronicdesign.com/communications/fundamentals-mimo[accessed on 9/09/2014].

[50] Eric T. Tchao, Kwasi Diawuo and W.K. Ofosu, "On the Comparison Analysis of 4G-WiMAX Base Station in an Urban Sub-Saharan African Environment", Journal of Communication and Computer October, 2013, pp 863-872, ISSN 1548-7709, USA.

[51] online:http://www.tutorialspoint.com/wimax/wimax_salient_features.htm [accessed on 4/05/2015].

Appendix A

Distance(m)	DL Throughput (Mbps)	UPLINK Throughput (Mbps)	Measured CINR (dB)	Measured RSSI(dBm)
4200	0.490	0.061	9	-73
4000	0.570	0.0200	2	-83
3900	0.541	0.054	-3	-87
3800	0.410	0.0264	-5	-92
3600	0.600	0.067	3	-81
3600	0.550	0.023	4	-87
3500	0.505	0.021	1	-79
3500	0.507	0.033	5	-78
3500	0.567	0.046	-4	-80
3300	0.505	0.097	2	-77
3200	0.540	0.084	0	-75
3000	0.590	0.031	5	-75
2800	0.300	0.315	-8	-73
2700	0.400	0.150	8	-74

2700	0.405	0.422	-7	-72
2000	2.01	1.61	6	-71
1900	1.2	0.122	11	-70
1800	1.25	1.04	10	-68
1600	1.5	1.33	13	`-67
1500	3.81	1.567	13	-67
1400	1.5	0.632	14	-65
1300	6.02	2.08	15	-69
1200	1.54	0.722	7	-70
1200	2.54	2.4	8	-65
1100	1.6	0.866	12	-64
900	1.35	0.802	14	-65
800	5.7	1.67	11	-63
800	3.2	2.05	7	-63
700	4.23	1.41	12	-60
700	3.3	2.06	6	-62
600	5.17	1.68	18	-55
570	4.66	1.43	21	-61
560	4.04	1.3	19	-57
550	4.75	0.846	23	-59
530	2.94	1.67	16	-57
520	5.17	1.24	18	-52

500	4.99	1.09	25	-61
500	4.81	1.72	40	-58
500	3.28	1.04	17	-62
470	3.31	1.22	24	-51
450	4.81	1.62	20	-59
420	4.91	1.65	30	-62
420	8.82	1.2	15	-51
415	3.84	1.08	24	-50
400	6.09	1.34	28	-61